Diplomarbeit

Eileen Radde, BSc

March 5, 2011

Eileen Radde, BSc

RASE – Replicative Assessment of Spectrometric Equipment Theoretical Description and Experimental Evaluation

MASTER THESIS

For obtaining the academic degree
Diplom-Ingenieurin

Master Programme of
Technical Physics

Graz University of Technology

Supervisor:

Univ.-Prof. Dipl.-Ing. Dr.techn. Helmuth Böck

Institute of Atomic and Subatomic Physics, Vienna University of Technology

Graz, February 2011

In Memoriam Peter Hafenscherer (1983-2008)

Acknowledgments

I would like to thank my supervisor Prof. Helmuth Böck for his help and patience. Without him, this work would have never been realised. I also want to thank Prof. Kindl, who encouradged me to go to Vienna. As this work was written in cooperation with the IAEA - Nuclear Security Unit, I want to thank the Unit, especially Michael Schrenk, who guided me through the 6 months at the NSU. I want to thank my family and friends, who always supported and motivated me over the whole period of my studies.

Contents

0.1 List of Figures

List of Figures

0.2 List of Tables

List of Tables

1 Theory[3,7,9]

The following section is a description of the basic theory. This description is mainly taken from the sources, G.F.Knoll, Radiation and Detection Measurement and the Lecture Course book of W.v.d.Linden, "Wahrscheinlichkeitstheorie, Statistik und Datenanalyse". The whole chapter is generally known and can be found in multiple books.

1.1 Radiation Principles

1.1.1 Radioactive decays

1. α - Decay

$$ {}^{A}_{Z}X \rightarrow {}^{A-4}_{Z-2}Y + {}^{4}_{2}\alpha $$

Heavy nuclei are energetically unstable and will therefore emitt a He-nucleus or α particle for stabilization. α - radiation is not very penetrating, in air the particles travel only a few cm, but they are heavily ionizing and can cause huge damage if they are incooperated.

2. β-Decay

- β^- - Decay

$$ {}^{A}_{Z}X \rightarrow {}^{A}_{Z+1}Y + \beta^- + \overline{\nu} $$

- β^+ - Decay

$$ {}^{A}_{Z}X \rightarrow {}^{A}_{Z-1}Y + \beta^+ + \nu $$

β-Radiation is a source for fast electrons. Most β- decays populate an excited state of the produced nucleus - so that γ - rays are emitted subsequently in the following de - excitation process (γ - radiation) as shown in figure 1. β - radiation can penetrate a few m in air and also the outer layers of skin.

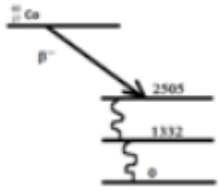

Figure 1: De - exitation process of β - Radiation

3. γ - Radiation

   It is emitted by excited nuclei in their transition to lower lying nuclear levels. These excited nuclear states are mostly created by a β - decay of a parent nuclide. The emitted energy is the energy difference between the initial and the final nuclear state. The energy of gamma rays are very specific as the energies of the nuclear states are also very well defined. The emission is nearly mono - energetic and the inherent line width of the photon energy distribution is nearly always small compared to the energy resolution of detectors.

1.1.2 Interactions of γ - rays with matter

A gamma ray spectrum can be produced by collecting all emitted gamma rays with a γ - spectrometry system. It contains in principle the number of γ -rays as a function of their energy. The shape of a spectrum comes from the interaction of the gamma rays with the detection volume. There are 3 main interacting effects: Pair production, Compton scattering and Photoelectric absorption. The effects are energy dependent which means, that in the area of interest for Nuclear Security purposes (up to 3000 keV) the photoelectric absorption effect is dominant. The energy dependence of the three effects is shown in figure 2.

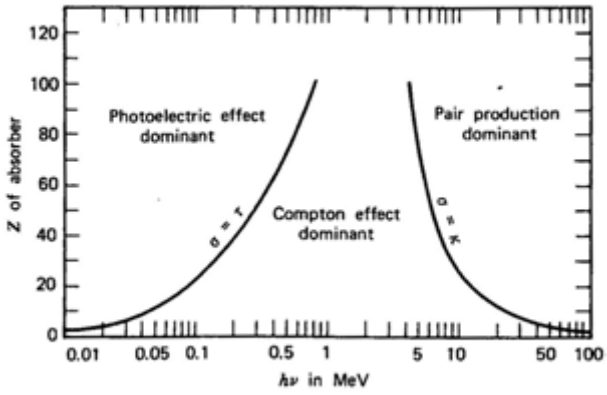

Figure 2: Energy dependence of the three interaction processes of γ - Radiation [3]

- Photo electric absorption

  An incoming photon is absorbed by an absorber atom, which emits an energetic photoelectron from its bound shells. Gamma ray photons produce electrons from K - shells. The electron carries the majority of the original photon energy.

$$E_e = h\nu - E_B$$

E_e is the energy of the electron, and E_B is the binding energy of the electron. The ionized atom will refill the vacancy by catching an electron from the medium or by a rearrangement of the electrons in the other shells. The photoelectric absorption process is heavily dependent on Z, meaning that the probability for the process is bigger for higher Z. As the process is dominant for gamma spectroscopy detectors, materials with high Z numbers are preferred.

- Compton Scattering

  This is the process between the incomming gamma ray photon and an electron of the absorbing material. The photon is scattered at the elctron and transfers a part of its energy (depending on the incoming angle) to the so called recoil electron. The probability for the Compton Scattering effect increases linearly with Z as there are more electrons available.

- Pair production

  If the energy exceeds twice the energy of an electron (1,02 MeV), the process of pair production is energetically possible. It is a dominant effect in higher energy ranges. The ineraction takes place in the Coulomb field of the nucleus, the gamma ray photon disappears and is replaced by an electron - positron pair. The resting energy goes into kinetic energy. The annihilation of the positrons yield to two photons, which can be detected sometimes in the gamma spectrum.

1.1.3 Gamma spectrometry - spectrum characteristics

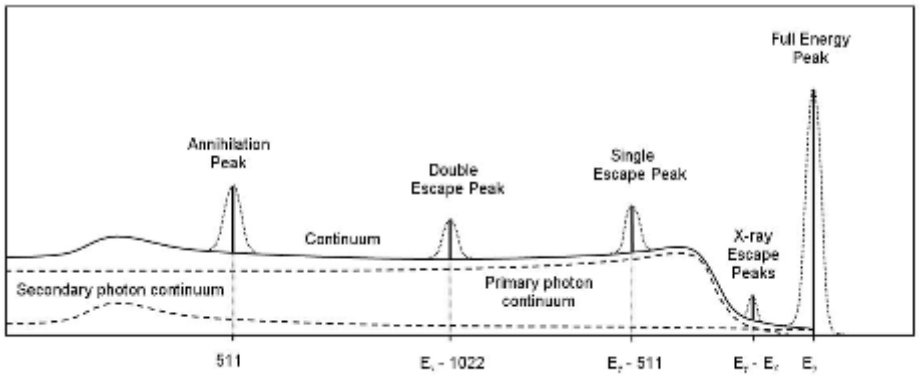

Figure 3: Draft of an ideal spectrum [3]

In figure 3 an ideal spectrum is displayed. There are several contributions to the spectrum, the background, the annihlation peak at 511 keV, the single and the double escape peak. Modern instruments are able to avoid displaying these effects. In the spectra of the modern instruments, which were used for this Master Thesis,

only the full energy and sometimes the X-ray escape peaks were important for this investigation. Another important parameter for the spectrum is the resolution. It is a general detector property, which is different for each detector. The resolution R is defined by:

$$R = \frac{FWHM}{E_0} \tag{1}$$

with E_0 the location of the centroid of the peak. In figure 4 the resoultion is shown.

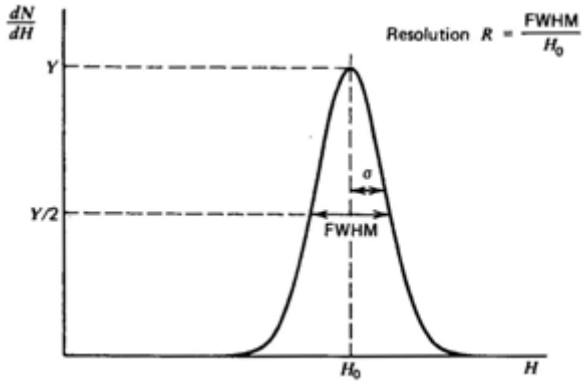

Figure 4: Resolution of a peak [3]

1.2 Gamma spectrometric equipment

For Nuclear Security purposes, there exist two main types of Gamma Ray Detectors.The first type is the scintillation detector, the second type is the high purity germanium detector.

1.2.1 Scintillation Detectors

Basically a scintallation detector collects scintillation light with high efficiency. Ideally it should convert the kinetic energy of the incomming particles with high efficiency into light. This conversion should be linear, meaning, that the light yield is proportional to the deposited energy. The crystal can either be organic or inorganic. The organic crystal is usually faster but has a less light output. Therefore it is better for neutron and β - radiation detection. The inorganic crystal consists of materials with high Z, and can therefore be used as γ - radiation detectors. The light output is produced by 3 processes, mainly the prompt fluorescence, which is the prompt emission of light after the excitation of the material. The two other processes are phosphorescences, meaning a larger and slower λ emission and the delayed fluorescence. If the detector is operated in pulse mode operation, only the prompt fluorescence is contributing to the light emission. In figure 5 the main interactions with the detector material are shown.

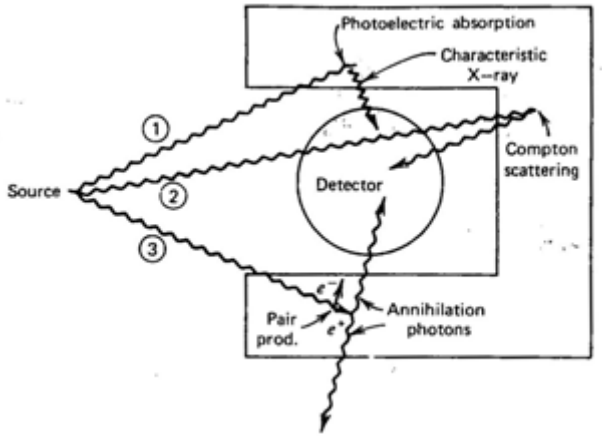

Figure 5: The main interactions contributing to the gamma spectrum [3]

1.2.2 Inorganic Detectors with Activators

In Nuclear Security one of the most used detectors is the NaI(Tl). It is part of the inorganic detectors, along with many other materials. The principle of function is

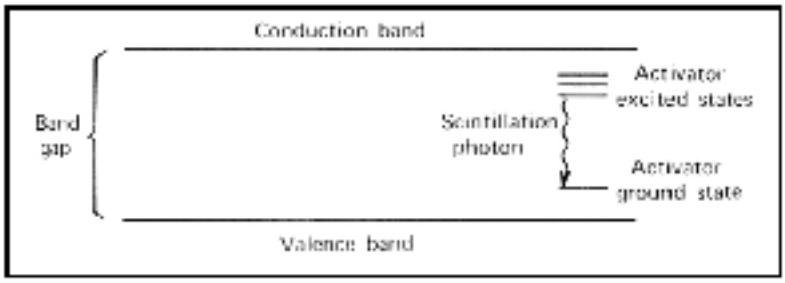

Figure 6: Activation of an electron to the Conduction Band [3]

quite easy.As shown in figure 6 an electron can be activated from the Valence band to the conduction band by absorbing more Energy then the Band Gap. In a pure crystal the return to the VB is either inefficient, or the size of the Bang Gap leads to an emission of light in a non visible range. If a small amount of impurities, a so called activator is added to the crystal, energy states in the Band Gap are created. The electron can now de - excite back to the Valence band. As the energy is now less then the original energy of the band gap, the emitted light is in the visible range. If a charged particle interacts with the detection volume, a large number of electron - hole pairs are created. The holes will drift to the activator sites, and ionize them. The electrons meanwhile can migrate freely through the crystal until they encounter an ionized activator. There they drop into the activator site, if de - exitation is possible, it will happen quickly, with a high probability of a photon emission.

- **NaI(Tl)** The dectector material was discovered in 1948 by R. Hofstadter. It is a quite cheap material which is the main advantage. The disadvantages are, that NaI is hygroscopic, fragile, sensitive to shocks and that it has a long decaying time of the scintillation pulse.

- $LaBr_3$**(Ce)** This material is the new alternative to NaI. It has a faster decay time, also a high Z, and a much better energy resolution. But La - 138 is a gamma emittor. The intrinsic radioactivity of the detector leads to a background of 1 - 2 counts $/cm^3 \times s$.

1.2.3 High Purity Germanium Detectors

Another widely used type of detector is the High Purity Germanium detector(HPGe). It's energy resolution is much better then the one of the $LaBr_3$ detector. As within a scintillation detector an incoming electron creates a whole chain of events to detect the created light in the scintillation material, not every event can be seen. The advantage of a semiconducting material is that an incident event creats a much larger number of carriers than any other detector material. The combination of a p and a n doped semiconducting material gives a junction diode(p- i- n). When a reverse bias is applied to the junction, the electrons and holes move to the adequate electrodes and a volume free of moving charge carriers (intrinsic volume) is produced. An incoming gamma quantum interacts with this non - conducting region and a proportional number of electrons to the gamma energy will be elevated to the respective electrode. The resulting current is then amplified and charges a capacitor. This signal is then digitalized and disturbing noise is filtered. To reduce thermal noise, which would lead to a permanent leakage current, the detector should be cooled to the temperature of liquid nitrogen (-195,79 Â°Celcius).

1.3 Nuclear Security[5]

The following threats were identified for Nuclear Security issues: "The threat involve criminals or terrorists acquiring and using for malicious purposes: (a) nuclear explosive devices, (b) nuclear material to build an improvised nuclear explosive device, (c) radioactive material to construct a radiological dispersal device (RDD) and/or (d) the dispersal of radioactivity through sabotage of installations in which nuclear and other radioactive material can be found or of such material in transport." Illicit trafficking is a part of this threat, by the prevention of illicit trafficking the threat could be reduced. Therefore it is one of the aims of the Nuclear Security Departement of the IAEA to prevent illicit trafficking of nuclear and other radioactive material. They have taken a number of steps: Nuclear and radiation safety legislation, Illicit Trafficking Database, Physical Protection of Nuclear Material, SSACs, Radiation safety, Prevention, detection and response, Training, Information Exchange and Analytical sevices. and also the surveillance of boarder crossings. Illicit trafficking means the unauthorized transport of decleared or undeclared radioactive material.

This can be a truck with scrap material, which carries radioactive sources without knowing. But this also includes malicious acts, like trafficking of materials for terrorist attacks. Radioactive sources are often deposited at scrap yards, some come from industrial uses (like nuclear gauges or for the weld inspections) others from medical uses. Another problem are the so called Orphan Sources, which are often found in former UdSSR states. To detect any of these sources and recycle or store them correctly and to prevent terrorist from their plans, different instruments are used.

- Portable Monitors

  They are used to scan trucks, cars, containers and people for gamma - ray sources. They usually consist of huge plastic scintillation detectors. Some of them are also able to identify the source.

- PRM - Personal Radiation Monitors

  These detectors are small like pagers, and can therefore be worn by the Front Line Officers (FLO) on the belt. They have small CsI or NaI crystals inside, which are very sensitive. They are together with the Portal Monitors the first detection level.

- RID - Radiation Identification Device

  These instruments cannot only alarm if gamma radiation is present (like the PRDs), they can also identify the source. These instruments are used after the verification of the alarm, to locate and identify the source present. Some instruments require experts use, like the HPGe, but most of the NaI can be used easily by the FLOs.

- NSD

  These instruments can localize neutron sources and should only be used by experts.

1.4 Statistical Significance Tests

Within these statistical analysis, indirect conclusions are drawn. One thinks, that the starting hypotheses is right. The significance niveau α is definded and it shows the critical range I_r^α:

$$P(z \in I_r^\alpha | H) = \alpha$$

If a measured value is in the critical range it's not accepted.

1.4.1 χ^2 - Test

This method is often used to compare measured values to theoretical values. There are so called controll factors $s_i \in \|R(i = 1, ..., N)$ which are used for experiments, the result of the experiments is d_i. There is a theoretical modell $y(s|a)$, which perdicts for the control factors s_i the measured values $y(s_i|a)$. The modell depends on the parameters a which are known. If the modell is rigth, the Zero Assumptions is that the measured values will not deviate more from the exact values than the measurement uncertainty.

$$d_i = y(s_i|a) + \eta_i$$

The deviations are normally distributed with known variance σ_i^2, which is either dependend on the control factors s_i or the exact values $y(s_i|a)$. The χ^2 statistics is then

$$x_0 = \sum_{i=0}^{N} \frac{(d_i - y(s_i|a))^2}{\sigma_i^2} \tag{2}$$

For a comparison of two value samples the χ^2 statistic can be calculated by the following:

$$\chi_0^2 = \sum_{l=1}^{L} \frac{(n_l - n_l^*)^2}{n_l^*} \tag{3}$$

The n_l^* are the theoretical values, the n_l the experimental values.

1.4.2 Comparison of Mean Values

With the t - test one can compare if the mean values of two control samples are equal. The conditons are:

- All variates are independent of each other.
- The variants in between the control samples are independent of each other.
- The variance is the same in both control samples.
- Zero - Hypotheses: The mean values are the same for both control samples.

The control samples $\{d_1^\beta, ..., d_{L_\beta}^\beta\}, (\beta = 1, 2)$ are the size of L_1 and L_2. The total number of the control samples is

$$L = L_1 + L_2$$

The mean values and the variances of the control samples are

$$\overline{d^{(\beta)}} = \frac{1}{L_\beta} \sum_{i=1}^{L_\beta} d_i^\beta$$

$$\overline{\Delta d(^{\beta})^2} = \frac{1}{L_\beta}\sum_{i=1}^{L_\beta}(d_i^\beta - \overline{d^\beta})^2$$

The Zero - Hypotheses says that the difference of the mean values of the control samples

$$\Delta = \overline{d^{(2)}} - \overline{d^{(1)}}$$

are normally distributed around zero. The estimated value for the variance of the difference Δ is

$$\widetilde{\sigma}^2 = \frac{L}{L^{(1)}L^{(2)}}(L^{(1)}\overline{(\Delta d^{(1)})^2} + L^{(2)}\overline{(\Delta d^{(2)})^2})$$

The t- statistics is

$$t = \frac{\Delta}{\widetilde{SF}} = \sqrt{L-2}\frac{(\overline{d^{(2)}}) - (\overline{d^{(1)}})}{\widetilde{\sigma}}$$

The degrees of freedom are $\nu = L - 2$. The calculation of the mean value leads to this decrease in the degrees of freedom. The test if two control samples with unknown variance have the same mean values is:
The factor

$$t = \sqrt{L-2}\frac{(\overline{d^{(2)}}) - (\overline{d^{(1)}})}{\widetilde{\sigma}} \tag{4}$$

$$\widetilde{\sigma} = \frac{L}{L^{(1)}L^{(2)}}(L^{(1)}\overline{(\Delta d^{(1)})^2} + L^{(2)}\overline{(\Delta d^{(2)})^2}) \tag{5}$$

is sufficient to the Student - t distribution

$$p_t(t|\nu) = \frac{\Gamma(\frac{\nu-1}{2})}{\Gamma(\frac{\nu}{2})}\frac{1}{\sqrt{\pi\nu}}(1+\frac{t^2}{\nu})^{-\frac{\nu+1}{2}} \tag{6}$$

with $\nu = L - 2$ degrees of freedom.

1.5 Semi - empirical approach for performance evaluation of radionuclide identifinders - Description [1]

Under the Coordinated Research Project M22007, *Development and implementation of instruments and methods for detection of unauthorized acts involving nuclear and other radioactive material* the IEAE, in cooperation with U.S. National laboratories, established an evaluation campaign to assess the performance of radiation detection equipment for nuclear security applications. The study targets instruments featuring radionuclide identification: spectrometric portal monitors, radionuclide identifiers, spectrometric portable radiation scanners, etc. The evaluation takes a semi - empirical approach, utilizing the instruments' replay and re- evaluation capabilities, also known as injection studies.
The challenge for the instruments is the identification of many different isotopes. Up to three isotopes have to be identified at the same time. The libraries have to be filled with a variety of nuclides, as there have to be a number of medical isotopes, all high risk nuclides, NORM materials and of course special nuclear material(SNM). The other challenge for the instruments is the presence of any influencing factors as shielding, masking or distortions due to temperature changes or the presence of a magnetic field. For the companies it is difficult to have on one side access to all demanded materials, but also to test the performance of the instrument with all these influences. Therefore the IAEA provides a semi - empirical test program to improve the performance of the instruments and to give a feedback to the companies. The program, RASE - Replicative Assessment of Spectrometric Equipment consists of six steps:

1. *Base spectra acquisition*

   A limited number of aggregate materials and sources containing high risk nuclides, spent fuel, nuclear materials and those nuclides frequently seen at international border crossings and other official points of entry (NORM and radiopharmaceuticals), are measured with high statistical accuracy. This shall be done in a laboratory environment, where effects due to temperature fluctuations and magnetic field variation are verified to be neglible. The sensitivity to material (fertilizer, ceramic tiles, lantern mantels, etc.) and sources are also to be measured in units of cps/(μSv/h). An investigation of the test materials will be done to determine the isotopic composition of the base material. The isotopic composition of the base composite materials will be determined independently prior to the evaluation with alternative techniques, such as mass and high resolution gamma spectrometry.

2. *Quantitative assessment of hardware tolerance*

   Distortion of the energy scale due to influencing factors will be assessed (see for example Fig.7) The first RASE cycle will adress the influence of high temperature, low temerature and constant magnetic field on energy calibration.

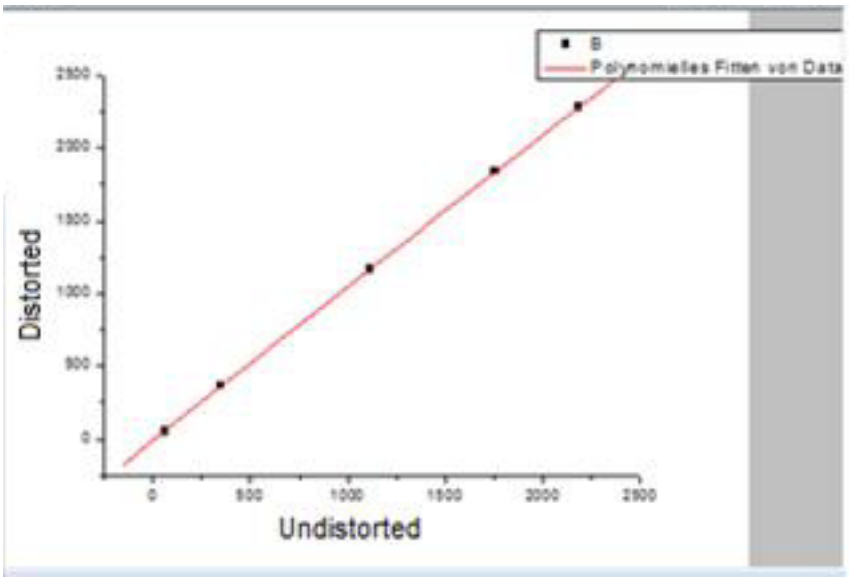

Figure 7: Distortion example [8]

Distortion of the response functions - resolution and pile up rejection efficiency will be taken into consideration on a later stage of study (see [8]).

3. *Replication*

   A large number of sample spectra will be replicated using the base spectra. The spectra will vary in several ways:

   - Specification of nuclide(s) of interest, aggregate radioactive material(s) (e.g. fractions), and background with partial contributions given in dose rate units;
   - Measurement (identification) time; and
   - Presence of influencing factor(s) - high/low temperature and magnetic field

   Each unique combination of nuclides will be associated with what is referred to here as a scenario file also containing the determined contributions by base spectra scaling, identification time, and the combination of a six - character alphanumerical code. The contents of the file will be encrypted.

4. *Injection and Identification*

   The sample spectra are injected into a manufacturer - provided PC - based identification software. This vendor - supplied executable code shall contain the same identification algorithm as that embedded in the instrument. Identification results from this executable code are recorded in the files, containing

the names of the source sample spectra. The names of the files with identification results will contain the name of the corresponding scenario, so that the RASE database manager can indicate the correctness of identification results under specific conditions.

5. *Identification results interpretation*

   At this step, an SQL - database is constructed from all identification results. The database name corresponds to the instrument and its model from which the base and sample are derived. The database contains the following elements:

   - First Nuclide
   - Its dose rate
   - Second Nuclide
   - Its dose rate
   - Third Nuclide
   - Its dose rate
   - Background dose rate
   - Identification time
   - Ambient temperature status (High, Low, Normal)
   - Magnetic field (Normal, High)
   - Number of false positive identifications
   - List of spurious nuclides
   - Number of false negative identifications
   - Number of false positives and false negative identifications
   - Average confidence index for the first nuclide

   Out of this range of data, the database manager can extract 2D or 3D ASCII data or excel spreadsheets for the results visualization.

6. *Validation*

   Two groups of validating tests are planned for RASE studies. The goal group of tst is to validate that the sample spectra correspond correctly to the sensitivity of the instrument within a statistical accuray. The second group of validation tests will prove the consistency and accuracy of the PC - based software in comparison with the firmware embedded in the instrument for a selected subset of experimental configurations.

1.5.1 Base spectra acquisition

The Base spectra acquisition is described in detail in the following chapter. For the ongoing steps it was necessary to treat all the spectra in a specific way. The spectra were taken with a high statistical accuracy that they can be downscaled later on. This process is also necessary to overlay two spectra. The downscaling process uses a random number generator (in MATLAB randn) which adds a noise to the spectrum. The first step is to adress in the Base spectrum characteristic points in each spectrum which are taken as base points. To these base points the noise is added. With the help of the Sensitivity parameter each dose rate can be generated this way. In equation 7 this process is described. Cs_0 is the spectrum with the base points, and the Background is added with an included noise. The first step for all spectra was the subtraction of the background of each spectrum. With this process the background was treated as a spectrum and can be added with each doserate to a spectrum.
A specific spectrum can be calculated as followed:

$$Cs_r = \lambda \times Cs_0 + (1 - \lambda) \times Bg \tag{7}$$

$$S = \frac{cps}{\mu Sv/h} \tag{8}$$

The RASE program offers a software to create synthetic spectra. To create these synthetic spectra the counts for the spectrum are needed. This can be calculated by the Sensitivity parameter. The user enters the Dose Rate and the time he wishes for the spectrum, this means that the only unknown parameter in the equation 8 is the cps. It can easily be transformed to the counts by multiplying it with the time. To overlay two or more spectra the following equation is used:

$$N_\Sigma(A) = \int (\Phi(E)+\Psi(E))G(E,A)dE = \int \Phi(E)G(E,A)dE + \int \Psi(E)G(A,E)dE = N_\Phi + N_\Psi(A) \tag{9}$$

In this equation the $N_\Psi(A)$, the $N_\Phi(A)$ and the $N_\Sigma(A)$ are the MCA spectra for the individual nuclides Ψ and Φ and their superposition Σ, $\Phi(E)$ and $\Psi(E)$ are the gamma energy spectra of the nuclides and the $G(E, A)$ is the instruments response function. Effects as self - shielding and non linear summation effects as dead time and sources self shielding are not included.
The second step with the hardware assesment was analysed by M. Gerstmayr in his Diploma theses see [8]. In the following chapter a detailed description of the Step One the Base spectra acquisition follows, as well as an analysis of the Sensitivity parameter calculation and an experimental evaluation of the overlaying spectra process.

2 Report of the RASE - Workshop at Seibersdorf and ATI in December 2009

2.1 Introduction

According to the Terms of Reference of the Semi-empirical approach for performance evaluation of radionuclide identifiers, RASE, the 1^{st} step of the RASE program is the base spectra acquisition. RASE is a new IAEA-driven program [1], [2], which utilizes a semi-empirical approach to study the performance of radionuclide identification equipment. The target instruments of these studies are Radionuclide Identification Devices, Portable Radiation Scanners, Spectrometric Radiation Portal Monitors in their wait-in operation mode, Spectrometric Personal Radiation Detectors or high resolution gamma spectrometers for isotopic composition assessment. The so called Base Spectra are Gamma Ray spectra of selected materials, taken with high statistical accuracy using the instruments of interest. For this purpose we used the following sources:

The Base spectra acquisition was prepared a week in advance, first measurements were taken to categorize the samples.

2.2 Objectives

The following report focuses only on the base spectra acquisition of the RASE program. The first objective of the step one was to acquire Base spectra of a limited number of high risk nuclides, spent fuel, nuclear materials and those nuclides frequently occurring at international border crossings and other official points of entry (NORM and radiopharmaceuticals) with high statistical accuracy. The spectra should be acquired under laboratory conditions, where effects due to temperature fluctuations and magnetic field variation are assumed to be negligible. The second objectives was the sensitivity measurement. The sensitivity to material and sources are to be measured in units of cps/(μSv/h). With the high statistical accuracy the participants are able to down scale the spectra later on, for further analysis of the instrument performance. The aim was to acquire spectra with 10^6 net counts.

No.	Isotope	Name	Activity	Calibration Date
1	Am - 241 - Li	N075	$4.07 * 10^{10}$Bq	01.06.1995
2	Cm - 244	02. Jun	$3.5 * 10^{8}$ Bq	15.02.2006
3	Cf - 252	E 8 - 282	3357380 Bq	01.02.2008
4	Eu - 154	738-64-2	373300	01.02.2001
5	LEU (19,9%) %	SU 135 19.9%		
6	U - 238 (3.1% enr.)	SU 136 3.1%		
7	Natural Uranium%	SU 137 0.7%		
8	Depleted Uranium%	SU 138 0.225%		
9	U - 235 89.99%	SU 145 89.99%		
10	Pu - 239 93%	SBNM - Pu 93		
11	Pu - 239 61%	SBNM - Pu 61		
12	Co - 60	1404 55-4	3785 Bq	01.12.2009
13	Co - 60	1404 55-5	38000 Bq	01.12.2009
14	Co 60	1404 55-6	385900 Bq	01.12.2009
15	Cs - 137			
16	Ir - 192	DP2-1-060/49/09/001	10MBq	09.12.2009
17	Co - 57			
18	Se - 75	DP2-1-050/49/09/001	10MBq	09.12.2009
19	Yb - 169	DP2-1-028/49/09/001	20MBq	09.12.2009
20	Tc - 99m			
21	Tl - 201			
22	Ga - 67			
23	I - 131			
24	Cs - 137			
25	Sr - 90	8921-003 ptw 19/77	33MBq	
26	Am - 241	126		1984
27	Ra - 226			
28	Th - 232			
29	K - 40	Fertilizer K 60, KO2		

Table 1: List of sources for the Base spectra acquisition

2.3 Experimental Setup

Eight vendors participated in the Base spectra acquisition, with 12 instruments. There were two experimental locations, one in Seibersdorf, the other at the Atominstitut of Vienna. These two locations were needed, as one of our tasks was to acquire spectra of fresh spent fuel, which can only be done at the Atominsitut. All the other acquisitions could be done in Seibersdorf, as all sources were present there. Depending on the location (Seibersdorf or Atominstitut) and the kind of the source the experimental setup was different. Three different kind of setups were used:

1. Container placed in Seibersdorf

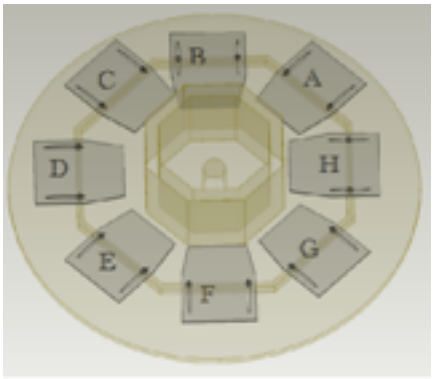

Figure 8: Draft of the container [M.Mayorov]

Figure 9: Container including lift and table

For sources no. 1- 14 the instruments were placed around a steel container. The inner steel wall had a thickness of 1 mm, and the outer steel wall 1.5 mm. The container was in the middle of a table with removable plates, so that the instruments could all be placed at the same distance to the source. Instruments were placed at a distance of 3 cm from the container. Figure 8 sketch a draft of the container, Figure 9 is a picture of the actual container.

The container was also placed on a lift, so that the height could be adjusted in accordance to the height of the source. The container was built to simulate a shipment container used to transport goods. This is an important condition to test, as the instruments examined in RASE are used in non proliferation and counter terrorism efforts to combat illicit trafficking of Nuclear Material.

2. Medical isotopes

Figure 10: Phantom

The second setup was for medical isotopes. These sources were placed in a so called "Phantom". It is important to distinguish in vivo versus ex vivo placed sources to reduce innocent alarms in border security applications(i.e. in vivo is not a trafficking threat). The Phantom is made of Plexiglas, its outer diameter is 202 mm, its inner diameter is 50 mm. The outer high is 222 mm, the inner high is 60 mm. The Phantom simulates a in - vivo source. The plexiglas is the simulation of human tissue.

3. Spent fuel

The third setup was for the spent fuel measurements at the Atominstitut. The fuel element had to be transported in a 20 cm lead shielding, a so called fuel transfer cask.It has in its middle exactly the place for one fuel element. This shielding was then placed on the fuel inspection unit. In figure 11 one

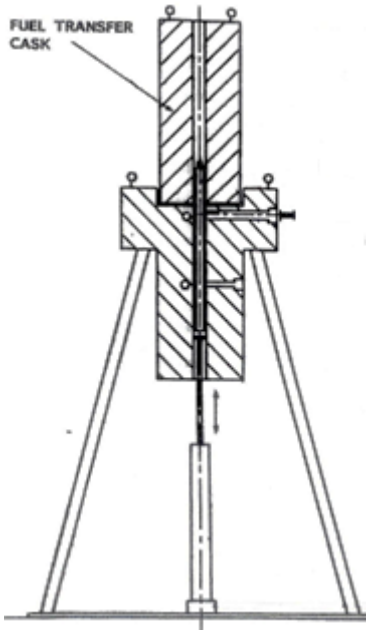

Figure 11: Draft of the fuel isnpection unit [11]

Figure 12: Procedure for spent fuel

can see the fuel inspection unit with the cask, Figure 12 shows the transport procedure. The instruments were placed in front of the fuel inspection unit.

2.3.1 Places and Instruments

place	Company	instrument
A	ORTEC	MicroDetective
		MicroDetective-HX
B	MIRION	SPIR Ident Pedestrian GN
C		SPIR ID LaBr3
		SPIR ID NaI
D	ICx	IdentiFINDER
		Interceptor
E	ASPECT	MKC-A03LB
F	CANBERRA	FALCON-5000
G		InSPECTOR-1000 L
H	ATOMTEX	AT6101C
		SPRD

Table 2: Places and Instruments

In table 2 there is a list of the instruments, which vendor provided which instrument and their positions around the container. The Interceptor from ICx and the SPRD from Atomtex were prototypes of new instruments. These instruments also took the spectra, but didn't participate in the RASE program as they are only in prototype phase.

2.3.2 Preparation of the Base Materials

Some materials had to be prepared in advance for the measurements. Most of the sources were ready for the measurements. However, potassium fertilizer for instance, had to be prepared. We bought 150 kg of potassium fertilizer, K 60, which is mainly KO_2, and distributed it equally into 16 bags. Then 2 of those 16 bags were put into 1 stronger bag, which fitted perfectly into the outer part of the container. Fig. 13 shows the fertilizer in the container.

Figure 13: Fertilizer in container

In addition the Ra - 226 samples had to be prepared for measurement. Radium stones were used as base material. These were put into plastic bags and later on into a plastic bottle, as one can see on the following pictures.

Figure 14: Radium stones

Ceramic tiles were in packages of 6, covered by a hard carton. These fitted perfectly into the outer part of the container.

Figure 15: Radium stones ready for measurement

Figure 16: Tiles ready for measurement

2.3.3 Preparation of the Measurements

One week before the workshop measurement preparations were preformed at Seibersdorf. This included also the count and dose rate measurement for sources no. 1, 2, 3, 5, 7, 8, 9, 10, 15, 17, 25, 26, 29 and the tiles.We used the pre-measurements to calculate the estimated time needed for each measurement at the workshop. During these measurements and during the workshop, we used 3 different kind of dosimeters for the dose and count rate measurements. These are described below.

Measurement equipment

- FLUKE Ionization Chamber
  This is an air ionization chamber capable measuring α,β and γ particles and calculating the dose rate. It has 349 cc of air inside, and a phenolic wall. The chamber window is Mylar. A graphite layer on the walls provides conduction. The FLUKE Ionization Chamber has quite a long measuring time, but with high accuracy. Highly active sources were measured with this detector.

Figure 17: FLUKE Ionization Chamber

- PRM 470 CGN
  The PRM 470 CGN is a Gamma and Neutron Radiation search device. We used it to measure the count rate of the sources at each location to make a correction of the dose rate. It has a $3,5' \times 2,88' \times 1,24'$ organic plastic scintillator for gamma radiation detection and a 4' ^3He tube for neutron radiation detection inside. This provides a 12,6 in^3 active volume. To have equivalent measurement times, we used the background update at the starting sequence to quantify the count rate. Each measurement lasted for 30 s.

Figure 18: PRM 470 CGN

- ATOMTEX 1125 AT
  The ATOMTEX 1125A was used to measure low dose rates. As the FLUKE Ionization chamber can preform quick and exact measurements only at high dose rates, we used the AT 1125A for sources with low activity. The AT 1125 A contains a NaI(Tl) crystal with a diameter of 25 × 40 mm. To get equal measurements we always restarted the measurement in front of a new source. The achievable limit of accuracy was less than 8% error. Sometimes, due to very low dose rates we had to stop the measurement at an error of 10%. To achieve the equal measurement of the dose rate, we used the setup shown in the Figure 19 below.

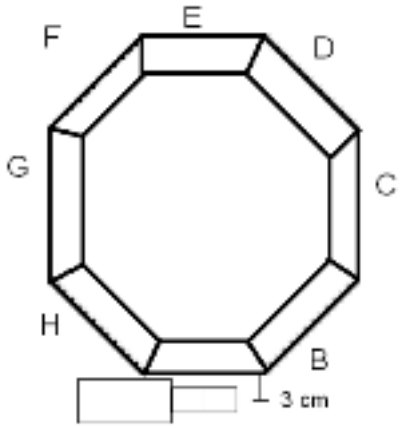

Figure 19: Dose rate measurement

Figure 20: ATOMTEX 1125A

2.3.4 Description of the Instruments

Vendors provided the equipment described in Table 2. The following section provides a short description of each instrument.

- Place A - ORTEC MicroDetective and ORTEC MicroDetective HX
  Both of these instruments are electrically cooled RIDs with High Purity Germanium Detectors. They have a 50×30 mm Germanium crystal inside. It's a p-type, coaxial crystal. For higher dose rates a Geiger Müller tube is incorporated. The only difference between these two instruments is the software. The HX is a newer model, and has therefore already included the newest demands of Nuclear Security.

- Place B - MIRION SpirIdent Pedestrian GN
  This instrument is a γ and neutron spectrometric portal monitor. It contains 2l NaI(Tl) tubes for γ radiation detection and nuclide identification and a ^{3}He tube for neutron detection.

- Place C - MIRION SpirIdent $LaBr_3$
  The SpirIdent $LaBr_3$ consists of a $1,5 \times 1,5'$ $LaBr_3$ crystal for γ radiation detection and nuclide identification and a ^{3}He tube for neutron detection. For high dose rates a Geiger Müller tube is incorporated.

Figure 21: The ORTEC MicroDetective and the MicroDetective Hx

Figure 22: MIRION portal monitor

- Place C MIRION SpirIdent NaI(Tl)
  The SpirIdent NaI(Tl) consists of a $3\times3'$ NaI(Tl) crystal crystal for γ radiation detection and nuclide identification and a ^{3}He tube for neutron detection. For high dose rates a Geiger Müller tube is incorporated.

Figure 23: The MIRION SpirIdent $LaBr_3$ and the NaI(Tl)

- Place D - ICx - IdentiFinder
  The ICx IdentiFinder has a $1,4' \times 2'$ NaI(Tl) crystal for γ radiation detection and nuclide identification and a ^{3}He tube for neutron detection. For high dose rates a Geiger Müller tube is incorporated.

Figure 24: ICx - IdentiFinder

- Place E - ASPECT MKC A03
  This instrument has a 40 × 40 mm NaI(Tl) crystal for γ radiation detection and nuclide identification and a ^{3}He tube for neutron detection. For high dose rates a Geiger Müller tube is incorporated.
- Place F - CANBERRA FALCON 5000
  This instrument is a High purity Germanium radionuclide identifier. The

Figure 25: ASPECT MKC A03

Germanium crystal (BE2380) is 60×30 mm. In addition this instrument has a Geiger Müller tube for high dose rate and a ^{3}He tube with an active volume of 24,8× 80 mm for neutron detection.

Figure 26: CANBERRA Falcon 5000

- Place G - CANBERRA Inspector 1000
  This instrument has a $1,5' \times 1,5'$ NaI(Tl) crystal for γ radiation detection. In addition there is a ^{3}He tube for neutron detection. For high dose rates a Geiger M"ller tube is incorporated.

- Place H - ATOMTEX Bagpack AT6101
  The ATOMTEX 6101 has a 63×63 mm NaI crystal as a γ radiation detector and for nuclide identification and a polyethylene moderated ^{3}He tube as a neutron detector.

Figure 27: CANBERRA Inspector 1000

Figure 28: ATOMTEX AT6101

2.3.5 Geometry of sources

Most of the sources could be placed in the middle of the container, and the instruments just around the source (no. 1-8, 10 - 24 and 25-29). These sources have a 4π Geometry. Sr - 90 and U - 235(90% enriched) sources only have a 2π Geometry. Therefore, these two sources were placed only at certain places of the container, and the instruments were put in front of these locations. The measurements were therefore performed consecutively. As a result there are only 1 - 2 count rate measurements and dose rate attributions for these sources.

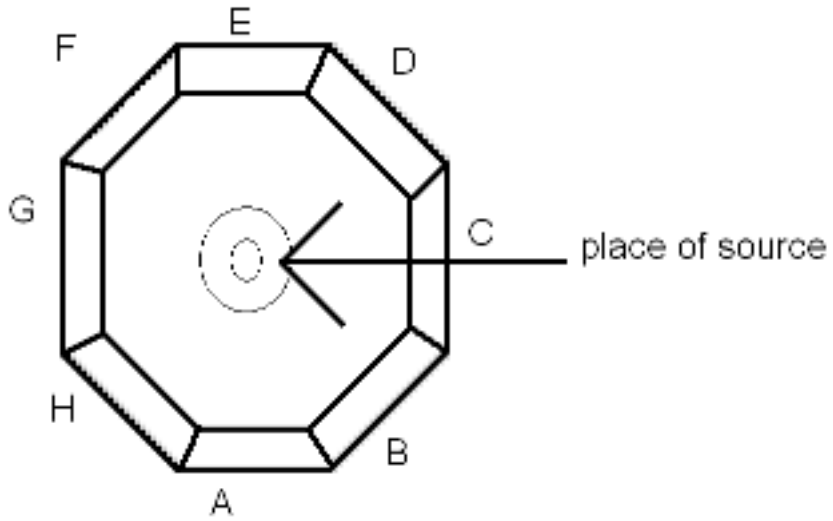

Figure 29: 4π Geometry

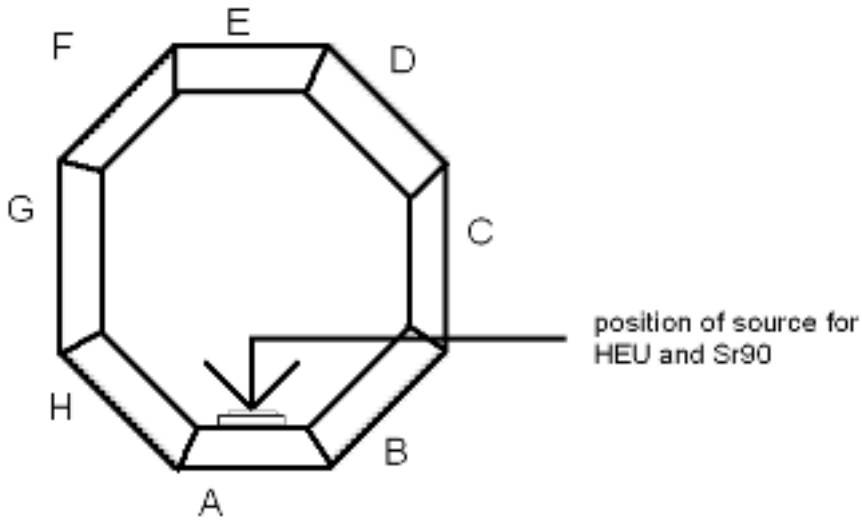

Figure 30: 2π Geometry

2.4 Experimental Procedures

2.4.1 Placement of instruments

The workshop began on Monday, 14^{th} of December 2009. Except one, all of the expected companies had arrived. In the morning all vendors recalibrated their instruments. Experts were in charge of one or two instruments, collecing all the data from the measurements at the end of the day. After the calibration of the instruments, the companies were asked to place their equipment at the designated position. There were no problems,exept for the MIRION portal monitor. We had to remove the table plate, and place the monitor in front of the containter. Figure 31 shows placement of the instruments.

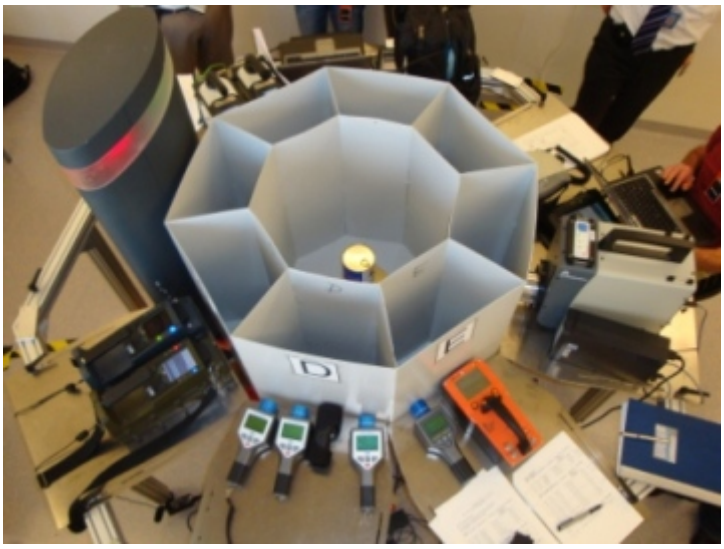

Figure 31: Placement of instruments

2.4.2 Measurement Procedure

The next step was to start the base spectra acquisition. Each source was placed in the center of the container. We had calculated in advance for each source the approximate time that would be needed to acquire 10^6 counts. Before the measurements of the participating instruments started, we took the dose rate at one or two places, and measured the count rate at each place around the container. With this procedure we were able to get the dose rate at each place, and so the sensitivity at each point.

2.4.3 Dose and Count rate Attribution

As already described, the count rate was measured with the PRM 470 CGN and the dose rate was measured with the ATOMTEX AT 1125A. If the dose rate was high we also cross checked the dose rate with the FLUKE Ionization Chamber. The tables below display for each source the date of the measurement, the measured time, the dose rate at certain points and the count rate at all points. As the portal monitor stood too close to the container, the cps measurement at point B wasn't possible. For later sensitivity calculations we took the mean value of the measurements at place A and C. The involved company did the same thing.

1. Measurement of Cm - 244

Date:	14.12.2009		
Start	10:30	Duration:	1800s
Material:	Cm - 244 02.2006		
Shielding:	Container		

Place	Dose rate[μ Sv/h]	Accuracy:	
G	0,242	6%	
F	0,22	6%	
FLUKE F	0,22		

Count rate (cps)							
A	B	C	D	E	F	G	H
734	681	733	711	755	737	768	720

Table 3: Cm - 244

2. Measurement of Cf - 252

Date:	14.12.2009		
Start:	11:15	Duration:	1980s
Material:	Cf - 252 E8-282		
Shielding:	Container		

Place	Dose rate[μ Sv/h]	Accuracy:	
E	0,54	8%	
D	0,54	8%	
FLUKE F	0,7		

Count rate (cps)							
A	B	C	D	E	F	G	H
995		1079	1051	1063	1003	965	945

Table 4: Cf - 252

3. Measurement of Am - Li

Date:	14.12.2009		
Start:	12:00	Duration:	120s
Material:	Am - Li N-075		
Shielding:	Container		

Place	Dose rate[μ Sv/h]	Accuracy:	
D	3,6	1%	
E	3,5	1%	
FLUKE E	3,9		

Count rate (cps)							
A	B	C	D	E	F	G	H
8742		9150	8616	9091	8388	8596	8098

Table 5: Am-Li

4. Measurement of LEU (19,9%)

Date:	14.12.2009		
Start:	12:30	Duration:	1980s
Material:	SU - 135 19.9 %		
Shielding:	Container		

Place	Dose rate[μ Sv/h]	Accuracy:	
D	0,31	1%	
FLUKE D	0,4		

Count rate (cps)							
A	B	C	D	E	F	G	H
1011		980	968	1020	1012	1031	965

Table 6: Low Enriched Uranium (19,9%)

5. Measurement of U - 238 3,1% enriched

Date:	14.12.2009		
Start:	13:15	Duration:	1980s
Material:	SU - 136 3.1%		
Shielding:	Container		

Place	Dose rate[μ Sv/h]	Accuracy:	
E	0,225	5%	
FLUKE D	0,29		

Count rate (cps)							
A	B	C	D	E	F	G	H
546		546	529	563	562	576	547

Table 7: Uranium 238, 3.1% enriched

6. Measurement of Natural Uranium

Date:	14.12.2009		
Start:	14:10	Duration:	2520s
Material:	SU - 137 0.7%		
Shielding:	Container		

Place	Dose rate[μ Sv/h]	Accuracy:	
E	0,218	5%	
G	0,205	5%	
FLUKE G	0,275		

Count rate (cps)							
A	B	C	D	E	F	G	H
444		460	473	476	443	445	411

Table 8: Natural Uranium

7. Measurement of Depleted Uranium

Date:	14.12.2009		
Start:	15:00	Duration:	2520s
Material:	SU - 138 0.225%		
Shielding:	Container		

Place	Dose rate[μ Sv/h]	Accuracy:	
E	0,204	6%	
FLUKE E	0,22		

Count rate (cps)							
A	B	C	D	E	F	G	H
456		448	430	441	435	452	439

Table 9: Depleted Uranium

8. Measurement of HEU 89,99%

Date:	14.12.2009		
Start:	16:00	Duration:	480s
Material:	SU - 145 89.99%		
Shielding:	Container		

Place	Dose rate[μSv/h]	Accuracy:	
E	0,51	4%	
D	0,51	4%	
B	0,5	5%	
H	0,5	5%	
FLUKE H	0,54		

Count rate (cps)							
A	B	C	D	E	F	G	H
	2176		2515	2577			2324

Table 10: High enriched Uranium

9. Measurement of the Background

Date:	14.12.2009		
Start:	17:00	Duration:	54000
Material:	Background		

Place	Dose rate[μ Sv/h]	Accuracy:	
D	0,048	8%	

Count rate (cps)							
A	B	C	D	E	F	G	H
69	69	70	66	68	66	78	73

Table 11: Background

10. Measurement of Plutonium 239 93%

Date:	15.12.2009		
Start:	08:50	Duration:	4020s
Material:	SBNM - Pu 93 93%		
Shielding:	Container	+ 1mm Cd	

Place	Dose rate[μ Sv/h]	Accuracy:	
E	0,1	8%	
H	0,11	8%	

Count rate (cps)							
A	B	C	D	E	F	G	H
248		252	252	265	258	267	233

Table 12: Plutonium 239 93%

11. Measurement of Plutonium 239 61%

Date:	15.12.2009		
Start:	10:15	Duration:	1800s
Material:	SBNM - Pu 61 61%		
Shielding:	Container	+ 1mm Cd	

Place	Dose rate[μ Sv/h]	Accuracy:	
E	0,23	6%	

Count rate (cps)							
A	B	C	D	E	F	G	H
577		609	627	618	632	597	575

Table 13: Plutonium 239 61%

12. Measurement of Co - 60

Date:	15.12.2009		
Start:	11:00	Duration:	2100s
Material:	Co 60		
Shielding:	Container		

Place	Dose rate[μ Sv/h]	Accuracy:	
E	0,61	6%	
H	0,61	6%	
FLUKE H	0,605		

Count rate (cps)							
A	B	C	D	E	F	G	H
514		549	550	580	560	549	512

Table 14: Co - 60

13. Measurement of Cs - 137 liquid

Date:	15.12.2009		
Start:	11:55	Duration:	420s
Material:	Cs - 137 liquid		
Shielding:	Container		

Place	Dose rate[μSv/h]	Accuracy:	
D	2,9	2%	

Count rate (cps)							
A	B	C	D	E	F	G	H
4896		4880	4785	4967	4898	4951	4758

Table 15: Cs - 137 liquid

14. Measurement of Ir - 192 liquid

Date:	15.12.2009		
Start:	12:15	Duration:	420s
Material:	Ir - 192 1l liquid		
Shielding:	Container		

Place	Dose rate[μSv/h]	Accuracy:	
D	1,28	2%	
H	1,33	2%	

Count rate (cps)							
A	B	C	D	E	F	G	H
3375		3454	3281	3296	3183	3266	3209

Table 16: Ir - 192 liquid

15. Measurement of Co - 57

Date:	15.12.2009		
Start:	12:35	Duration:	2700s
Material:	Co - 57		
Shielding:	Container		

Place	Dose rate[μSv/h]	Accuracy:	
D	0,088	6%	

Count rate (cps)							
A	B	C	D	E	F	G	H
344		333	328	328	325	333	338

Table 17: Co - 57

16. Measurement of Se - 75 liquid

Date:	15.12.2009		
Start:	13:35	Duration:	1980s
Material:	Se - 75 1l liquid		
Shielding:	Container		
Place	Dose rate[μ Sv/h]	Accuracy:	
D	0,185	5%	

Count rate (cps)							
A	B	C	D	E	F	G	H
522		539	506	541	539	555	523

Table 18: Se - 75 liquid

17. Measurement of Yb - 169 liquid

Date:	15.12.2009		
Start:	14:30	Duration:	4020s
Material:	Yb - 169 1l liquid		
Shielding:	Container		
Place	Dose rate[μ Sv/h]	Accuracy:	
F	0,086	4%	

Count rate (cps)							
A	B	C	D	E	F	G	H
224		219	206	208	208	219	217

Table 19: Yb - 169 liquid

18. Measurement of tiles

Date:	15.12.2009		
Start:	15:50	Duration:	57600
Material:	tiles		
Shielding:	container		

Place	Dose rate[μSv/h]	Accuracy:	
D	0,086	8%	

Count rate (cps)							
A	B	C	D	E	F	G	H
143		136	136	103	136	146	121

Table 20: Tiles

19. Measurement of Tc - 99m

Date:	16.12.2009		
Start:	09:15	Duration:	180s
Material:	Tc - 99m		
Shielding:	Phantom		

Place	Dose rate[μSv/h]	Accuracy:	
D	1,29	1%	

Count rate (cps)							
A	B	C	D	E	F	G	H
6187		5928	5333	5416	5439	5843	6016

Table 21: Tc - 99m

20. Measurement of Tl - 201

Date:	16.12.2009		
Start:	09:30	Duration:	480s
Material:	Tl - 201		
Shielding:	Phantom		

Place	Dose rate[μSv/h]	Accuracy:	
A	0,68	2%	
FLUKE A	0,75		

Count rate (cps)							
A	B	C	D	E	F	G	H
2103		1971	1932	1931	1929	2024	2040

Table 22: Tl - 201

21. Measurement of Ga - 67

Date:	16.12.2009		
Start:	09:50	Duration:	420s
Material:	Ga - 67		
Shielding:	Phantom		

Place	Dose rate[μSv/h]	Accuracy:	
D	0,8	2%	
FLUKE	0,8		

Count rate (cps)							
A	B	C	D	E	F	G	H
3060		2953	2948	3044	3045	3075	3007

Table 23: Ga - 67

22. Measurement of I - 131

Date:	16.12.2009		
Start:	10:10	Duration:	480s
Material:	I - 131		
Shielding:	Phantom		

Place	Dose rate[μSv/h]	Accuracy:	
D	0,87	2%	

Count rate (cps)							
A	B	C	D	E	F	G	H
3098		2867	2743	2757	2683	2826	2970

Table 24: I - 131

23. Measurement of Cs - 137 and I - 131

Date:	16.12.2009		
Start:	10:30	Duration:	240s
Material:	I - 131 (0.87 μSv/h)	+ Cs - 137	
Shielding:	Phantom for I - 131	none for	Cs - 137

Place	Dose rate[μ Sv/h]	Accuracy:	
D	1,52	1%	

Count rate (cps)							
A	B	C	D	E	F	G	H
4478		4287	4044	4093	4109	4254	4371

Table 25: I - 131 and Cs - 137

24. Measurement of Cs - 137

Date:	16.12.2009		
Start:	10:45	Duration:	660s
Material:	Cs - 137		
Shielding:	none		

Place	Dose rate[μ Sv/h]	Accuracy:	
D	0,71	3%	

Count rate (cps)							
A	B	C	D	E	F	G	H
1594		1456	1431	1430	1458	1509	1552

Table 26: Cs - 137

25. Measurement of Sr - 90

Date:	16.12.2009		
Start:	11:10	Duration:	300s
Material:	Sr - 90		
Shielding:	Container		

Place	Dose rate[μ Sv/h]	Accuracy:	
E	1,48	2%	
B	0,175	6%	1m distance

Count rate (cps)							
A	B	C	D	E	F	G	H
				5294			

Table 27: Sr - 90

26. Measurement of Am - 241

Date:	16.12.2009		
Start:	12:25	Duration:	420s
Material:	Am - 241		
Shielding:	Container		

Place	Dose rate[μSv/h]	Accuracy:	
D	0,52	3%	

Count rate (cps)							
A	B	C	D	E	F	G	H
1021		931	872	878	835	927	933

Table 28: Am - 241

27. Measurements of Radium Stones

Date:	16.12.2009		
Start:	12:45	Duration:	3600s
Material:	Ra - 226 stone		
Shielding:	Container		

Place	Dose rate[μ Sv/h]	Accuracy:	
D	0,21	6%	

Count rate (cps)							
A	B	C	D	E	F	G	H
308	297	282	290	304	298	328	307

Table 29: Radium Stones

28. Measurement of Th - 232

Date:	16.12.2009		
Start:	14:10	Duration:	1200s
Material:	Th - 232		
Shielding:	Container		

Place	Dose rate[μ Sv/h]	Accuracy:	
E	0,77	4%	
FLUKE D	0,85		

Count rate (cps)							
A	B	C	D	E	F	G	H
1080		1093	897	1011	933	895	781

Table 30: Th - 232

29. Measurement of Eu - 154

Date:	16.12.2009		
Start:	15:05	Duration:	1500s
Material:	Eu - 154 738-64-2		
Shielding:	Container		

Place	Dose rate[μSv/h]	Accuracy:	
E	0,218	5%	

Count rate (cps)							
A	B	C	D	E	F	G	H
332		325	300	321	323	326	329

Table 31: Eu - 154

30. Measurement of Potassium Fertilizer

Date:	16.12.2009		
Start:	15:50	Duration:	57600
Material:	K fertilizer K60, KO2		
Shielding:	Container		

Place	Dose rate[μSv/h]	Accuracy:	
D	0,242	5%	

Count rate (cps)							
A	B	C	D	E	F	G	H
290		248	232	243	257	281	277

Table 32: Potassium Fertilizer

31. Background Measurement at the Atominstitut Higher background due to

Date:	17.12.2009		
Start:	10:00	Duration:	3600s
Material:	Background at ATI		
Shielding:	none		

Dose rate (away from reactor):	410 nSv/h	Accuracy: 5 %
Dose rate (to reactor):	550 nSv/h	Accuracy: 5 %

Table 33: Background at Atominstitut

reactor in operation.

3 Results of Step One - Base spectra acquisition

The aim was to acquire spectra with a high statistical accuracy. The previous chapters described these procedures. After the workshop all data and spectra were gathered. The dose rate was calculated at each point, with the cps measurements. After obtaining the dose rate at each point, the Sensitivity parameter was determined which is given by equation 8.
In the tables 3 to 3 one can find the equivalent dose rate for each instrument and location, which was calculated from our data. The background was subtracted later on and the Sensitivity S was calculated. As the background should always kept the same for each ongoing procedure, the background has to be subtracted. It can be added to the individual background spectra. The instruments were those described in previous sections. The abbreviations are

- MKC - MKC-A03LB of ASPECT
- ICX - IdentiFINDER
- PORTAL - MIRION Portal Monitor
- MIRNaI - NaI - detector instrument of MIRION
- MIRLaBr - MIRION's $LaBr_3$ detector.
- ORTEC 1 - MicroDetective
- ORTEC 2 - MicroDetective- HX

Instrument	Cm-244	Cf-252	Am-Li	SU 135	SU 136	SU 137	SU 138	SU 145
	[μSv/h]	[μSv/h]	[μSv/h]	[μSv/h]	[μSv/h]	[μSv/h]	[μSv/h]	[μSv/h]
MKC	0,18	0,49	3,75	0,28	0,21	0,17	0,15	0,46
ATOMTEX	0,17	0,43	3,33	0,26	0,19	0,14	0,15	0,45
FALCON	0,18	0,46	3,45	0,28	0,21	0,16	0,15	0,45
INSPECTOR	0,18	0,43	3,53	0,27	0,20	0,15	0,15	0,44
ICX	0,17	0,49	3,55	0,26	0,19	0,17	0,15	0,46
PORTAL	0,16	0,48	3,68	0,27	0,20	0,16	0,16	0,45
MIRNaI	0,17	0,50	3,77	0,26	0,20	0,16	0,16	0,45
MIRLaBr	0,17	0,50	3,77	0,26	0,20	0,16	0,16	0,45
ORTEC1	0,18	0,46	3,60	0,27	0,20	0,15	0,16	0,45
ORTEC2	0,18	0,46	3,60	0,27	0,20	0,15	0,16	0,45

Table 34: Dose rate data of all sources and instruments of the first day of the workshop

After the end of the first day, a long overnight background measurements were taken. The cps data were taken in advance and the dose rate was calculated afterwards.

Instrument	Bgnd
	[μSv/h]
MKC	0,05
ATOMTEX	0,05
FALCON	0,05
INSPECTOR	0,06
ICX	0,05
PORTAL	0,05
MIRNaI	0,05
MIRLaBr	0,05
ORTEC 1	0,05
ORTEC 2	0,05

Table 35: Dose rate of the background measurement after the first day

Instrument	WGPu 93	RGPU61	Co-60	Ir-192	Co-57	Se-75	Yb-169	Ceram
	[μSv/h]	[μSv/h]	[μSv/h]	[μSv/h]	[μSv/h]	[μSv/h]	[μSv/h]	[μSv/h]
MKC	0,05	0,18	0,56	1,28	0,18	0,15	0,04	0,02
ATOMTEX	0,03	0,16	0,56	1,24	0,17	0,14	0,04	0,02
FALCON	0,05	0,19	0,57	1,23	0,18	0,15	0,04	0,04
INSPECTOR	0,04	0,17	0,55	1,26	0,18	0,15	0,03	0,04
ICX	0,05	0,19	0,56	1,27	0,17	0,14	0,04	0,04
PORTAL	0,04	0,17	0,54	1,32	0,16	0,14	0,04	0,04
MIRNaI	0,04	0,18	0,56	1,34	0,17	0,15	0,04	0,04
MIRLaBr	0,04	0,18	0,56	1,34	0,17	0,15	0,04	0,04
ORTEC1	0,04	0,16	0,52	1,31	0,18	0,14	0,04	0,04
ORTEC2	0,04	0,16	0,52	1,31	0,18	0,14	0,04	0,04

Table 36: Dose rate data of all sources and instruments of the second day

Instrument	Tc-99m	Tl-201	Ga-67	I-131	Cs-137	Sr-90
	[μSv/h]	[μSv/h]	[μSv/h]	[μSv/h]	[μSv/h]	[μSv/h]
MKC	1,26	0,57	0,78	0,83	2,96	1,43
ATOMTEX	1,40	0,61	0,76	0,89	2,83	1,43
FALCON	1,27	0,58	0,78	0,80	2,92	1,43
INSPECTOR	1,36	0,60	0,78	0,84	2,94	1,42
ICX	1,24	0,58	0,75	0,82	2,85	1,43
PORTAL	1,42	0,61	0,77	0,90	2,91	1,43
MIRNaI	1,38	0,59	0,75	0,86	2,91	1,43
MIRLaBr	1,38	0,59	0,75	0,86	2,91	1,43
ORTEC1	1,45	0,63	0,78	0,93	2,92	1,43
ORTEC2	1,45	0,63	0,78	0,93	2,92	1,43

Table 37: First part of the dose rate data of all sources and instruments of the third day

Instrument	Am-241	Ra-226	Th-232	Eu-154	Fert
	[μSv/h]	[μSv/h]	[μSv/h]	[μSv/h]	[μSv/h]
MKCA03	0,47	0,17	0,72	0,17	0,20
ATOMTEX	0,50	0,17	0,54	0,17	0,24
FALCON	0,45	0,17	0,66	0,17	0,22
INSPECTOR	0,50	0,18	0,62	0,16	0,24
ICX	0,47	0,16	0,64	0,16	0,19
MIRNaI	0,53	0,16	0,78	0,17	0,23
MIRLaBr	0,53	0,16	0,78	0,17	0,23
PORTAL	0,50	0,15	0,78	0,17	0,21
ORTEC001	0,56	0,17	0,77	0,18	0,25
ORTEC002	0,56	0,17	0,77	0,18	0,25

Table 38: Second part of the dose rate data of all sources and instruments of the third day

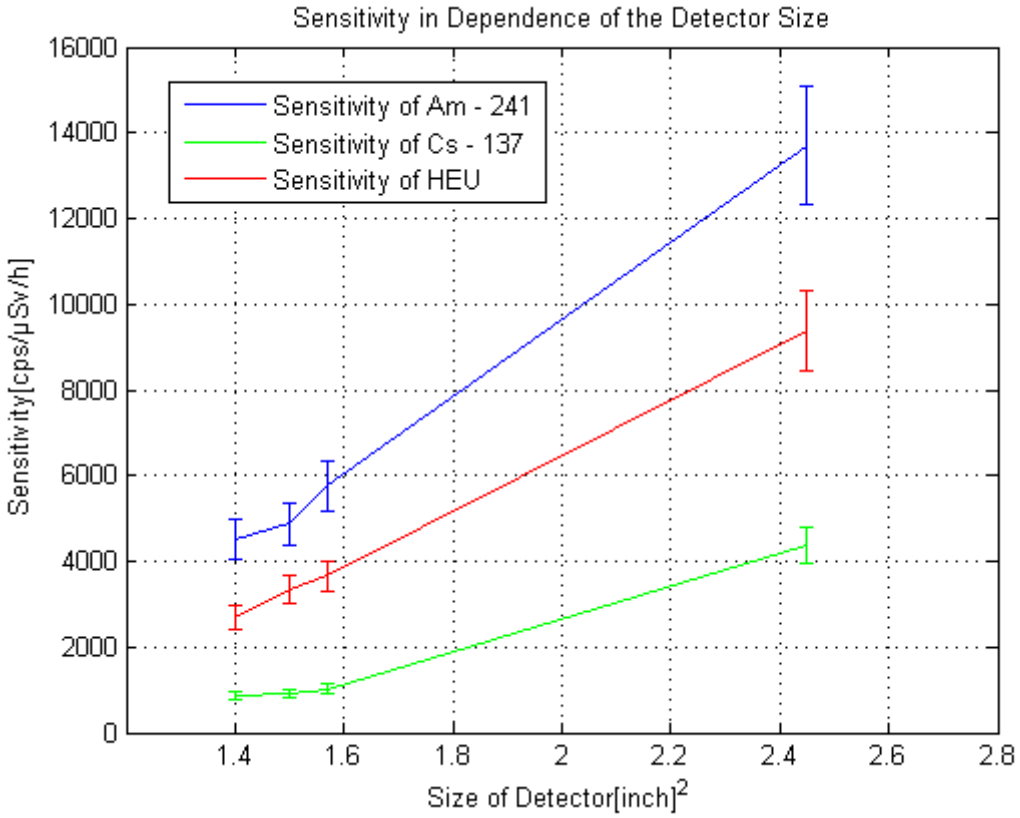

Figure 32: Sensitivity of the detectors compared by their front area

In figure 32 the difference of the sensitivity depending on the detector front area size is displayed. For the comparison 3 different kind of sources were chosen, each of the sources have different characteristics in its spectra. As the Am - 241 is a high energetic source, it has the highest sensitivity. The Cs - 137 is a lower energetic source, so the sensitivity of the source is lower. To get 0.1 μSv/h you need 10^4 cps with a Am - 241 source, but only 500 cps with a Cs - 137 source. This Cs - 137 source can harm people more than this Am - 241 source. As one can see in figure 33 the comparison by the volume of the detector is not as accurate as the comparison by the front area size. It seems, that the front area size has more influence in the sensitivity of the detector as the volume of the detector.
In the following figures the difference between the different kind of detectors is shown. One can see in fig. 34 and in fig. 35 the difference in the shape of the spectrum quite well. The two sources were Cs - 137 and HEU.

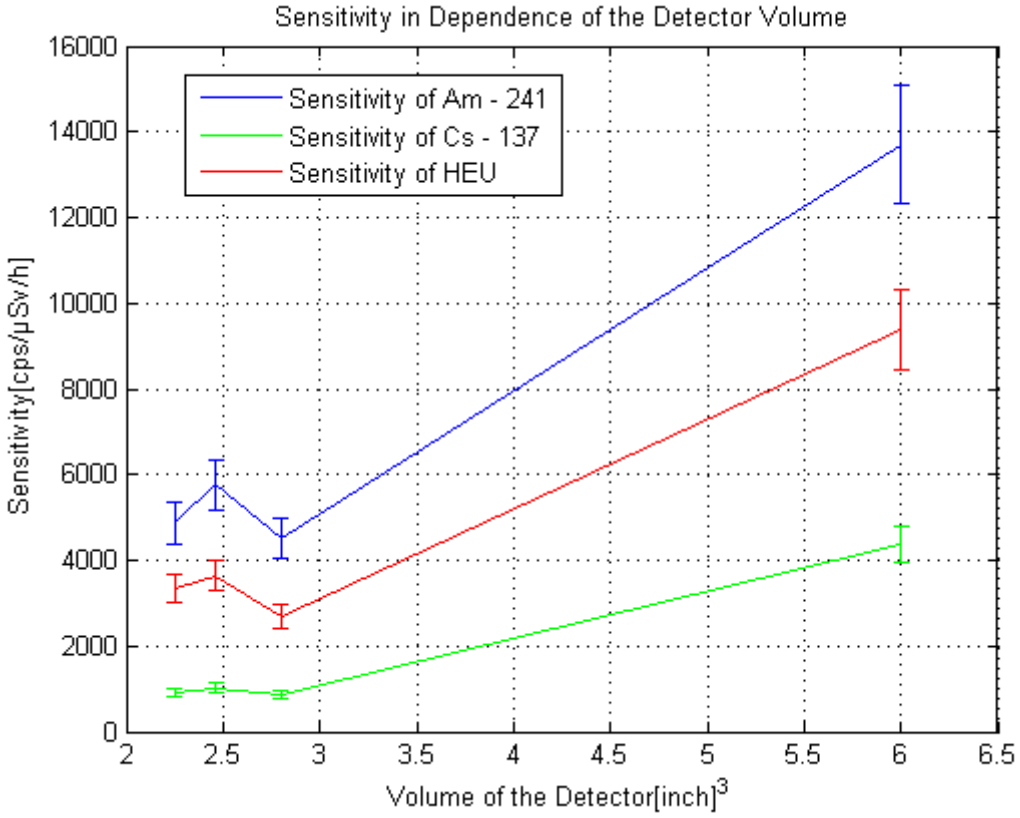

Figure 33: Sensitivity of detectors compared by their volume

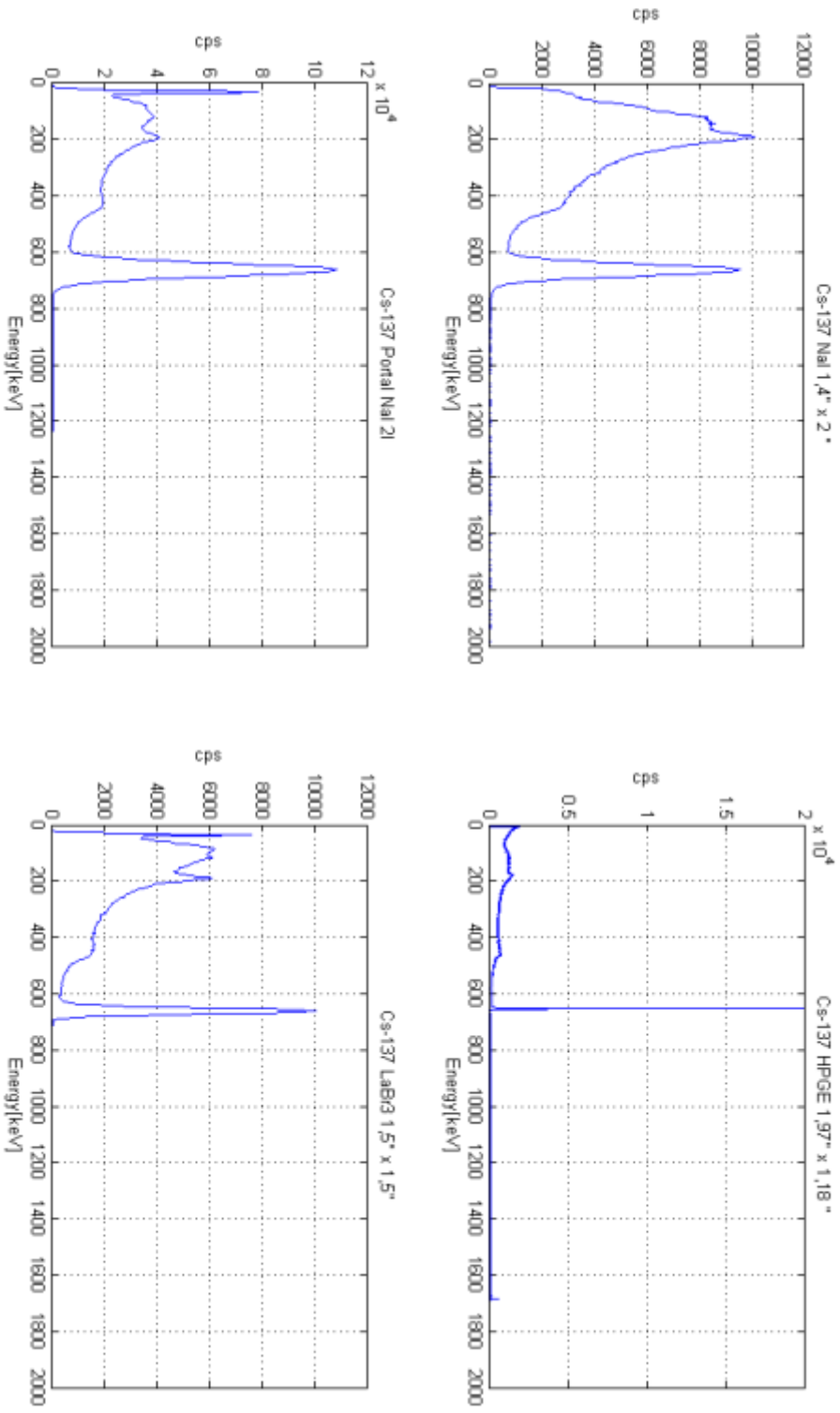

Figure 34: Cs - 137 comparison between different detectors

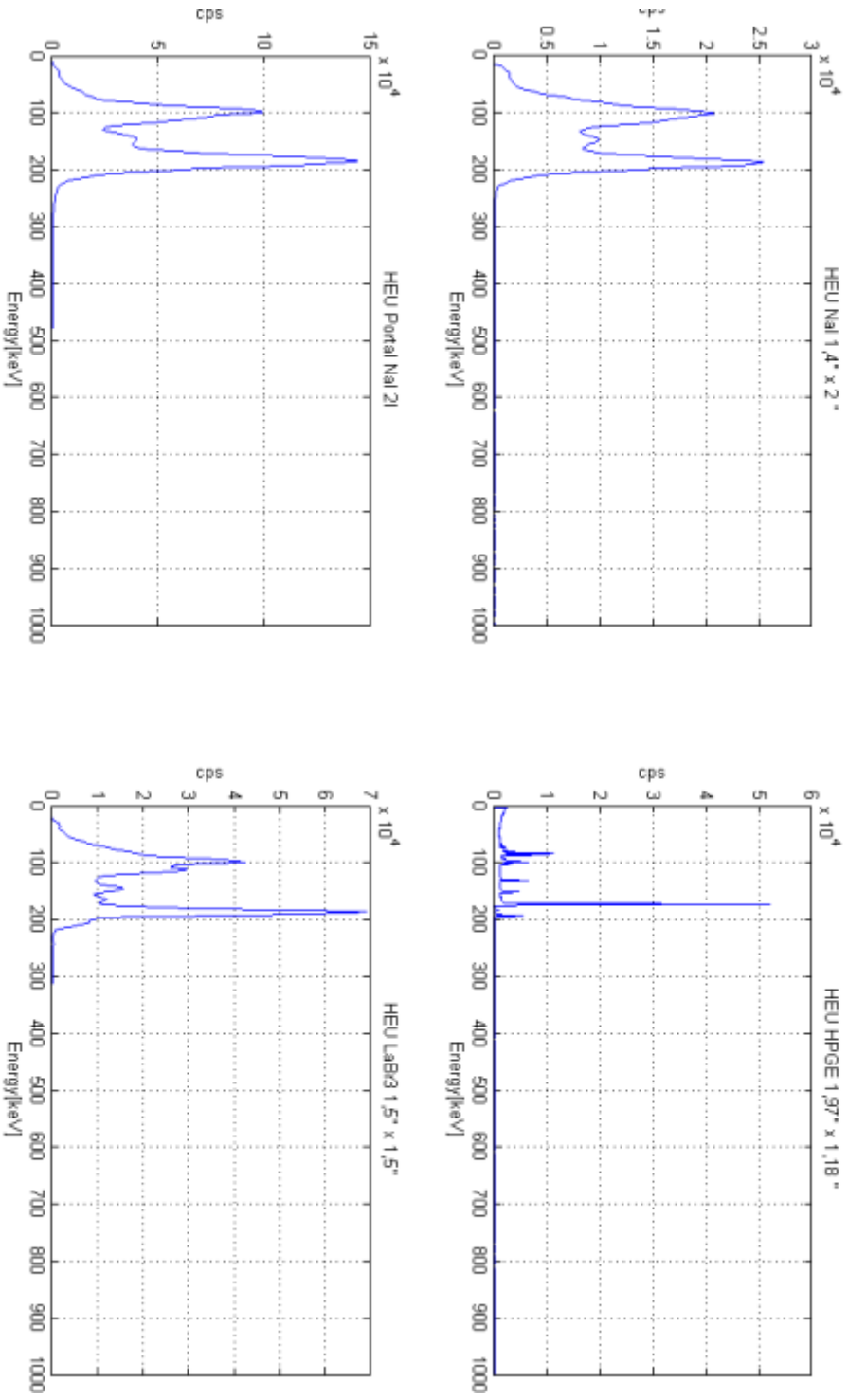

Figure 35: Comparison of different detectors for HEU

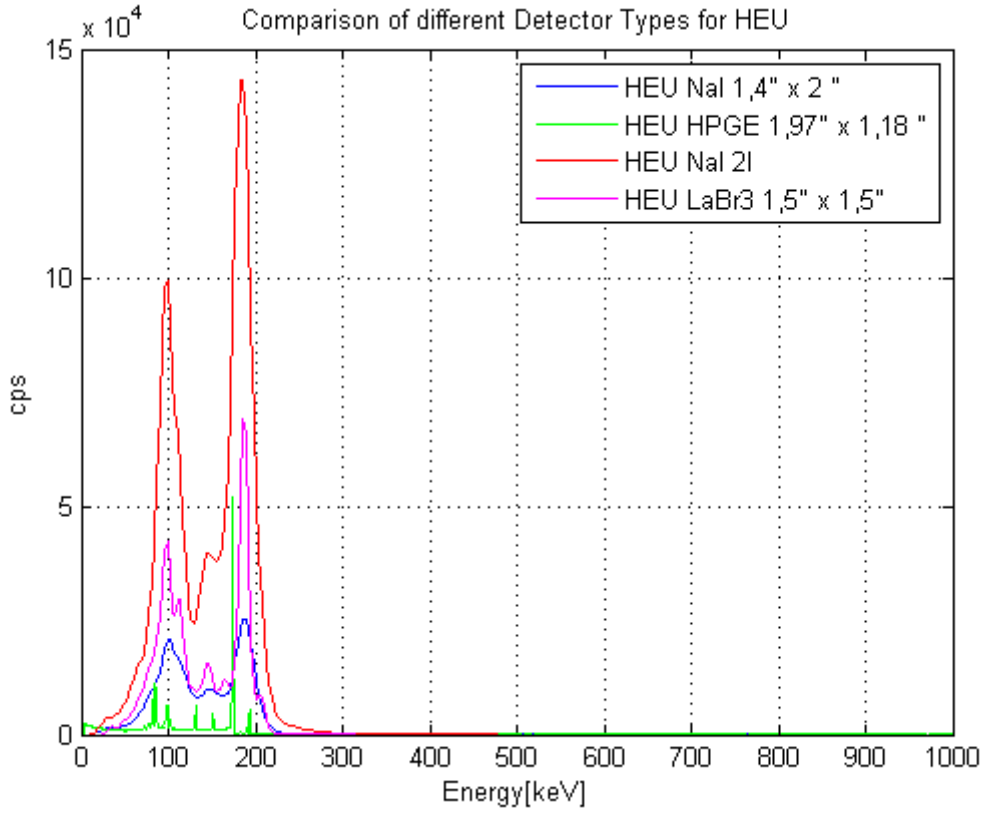

Figure 36: Comparison of 4 different detectortypes for HEU

Figures 36 and 37 show the direct comparison between the detectors for 2 sources. All spectra were acquired in the same time. In figure 38 and 39 all spectra are shown in logarithmic scale to display out the differences between the detectors, especially between the HPGe and the others.
The two NaI Detectors show almost the same resolution (around 7 %). The different detector size is obvious. The portal monitor is equipped with a larger detector, and can therefore gather more counts in the same time than the IdentiFINDER. This detector cannot show all peaks. The opposite example is the High Purity Germanium Detector, which displays all peaks, with a very good resolution. As the detector size is quite small, it has a much lower count rate, and compared to the NaI it has a much higher dead time (around 20%).
An alternative is the $LaBr_3$ - Detector. A resolution around 3 %, a dead time around 1 - 2 %, showing all the peaks. There is something else remarkable in these spectra: Cs - 137 has always a 32keV peak, that should still be seen in the spectra. In this comparison you can see this peak only with the Portal Monitor and the $LaBr_3$ - detector. The spectra of the two other instruments do not show the peak. For the IdentiFINDER it seems that the Low Level Discriminator was set too high. Most of the instruments use a cap over their detector, which can absorbe this 32 keV peak.

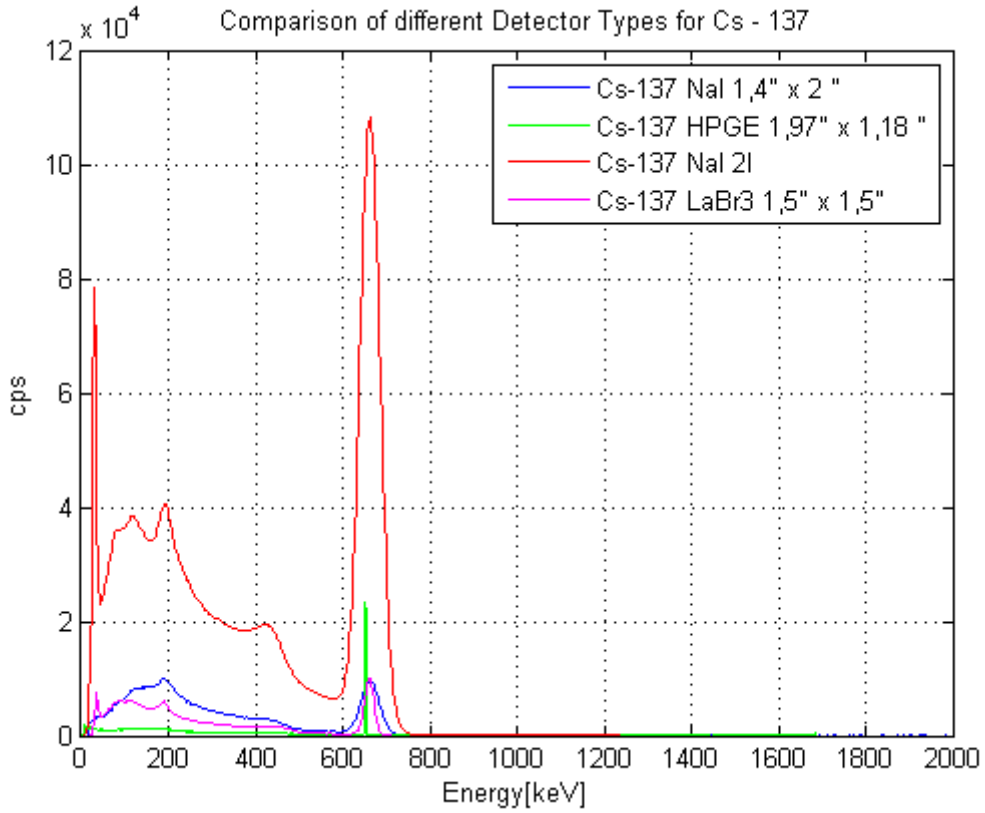

Figure 37: Comparison of 4 different detectortypes for Cs - 137

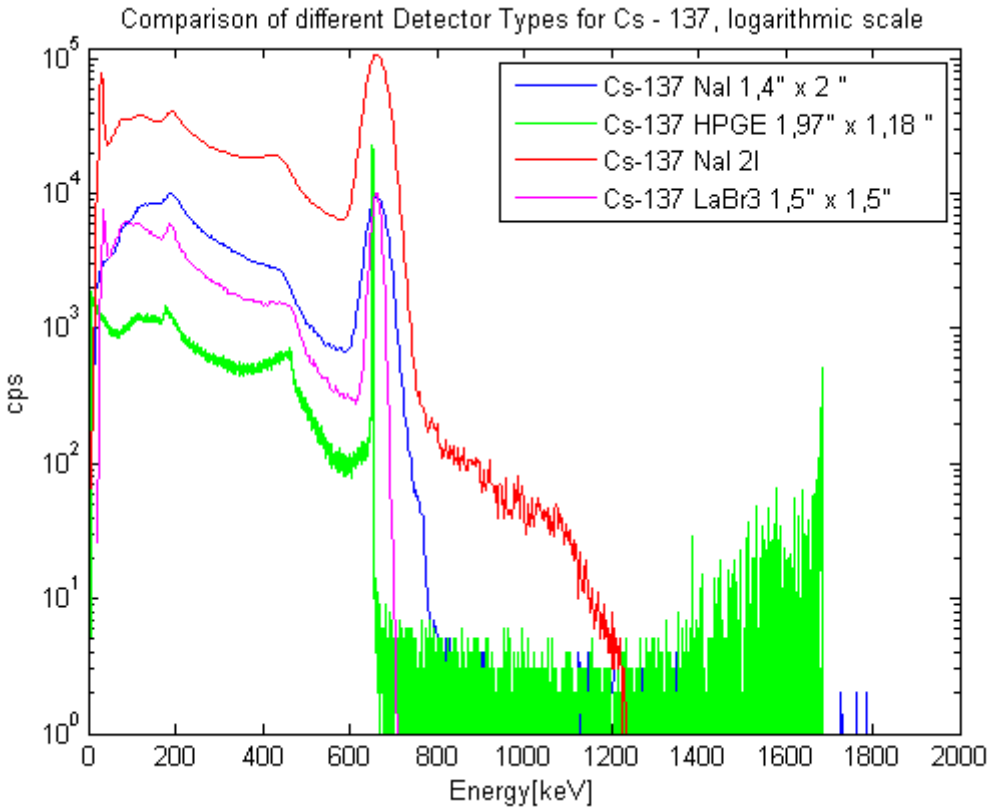

Figure 38: Comparison of 4 differnet detectortypes for Cs - 137 in logarithmic scale

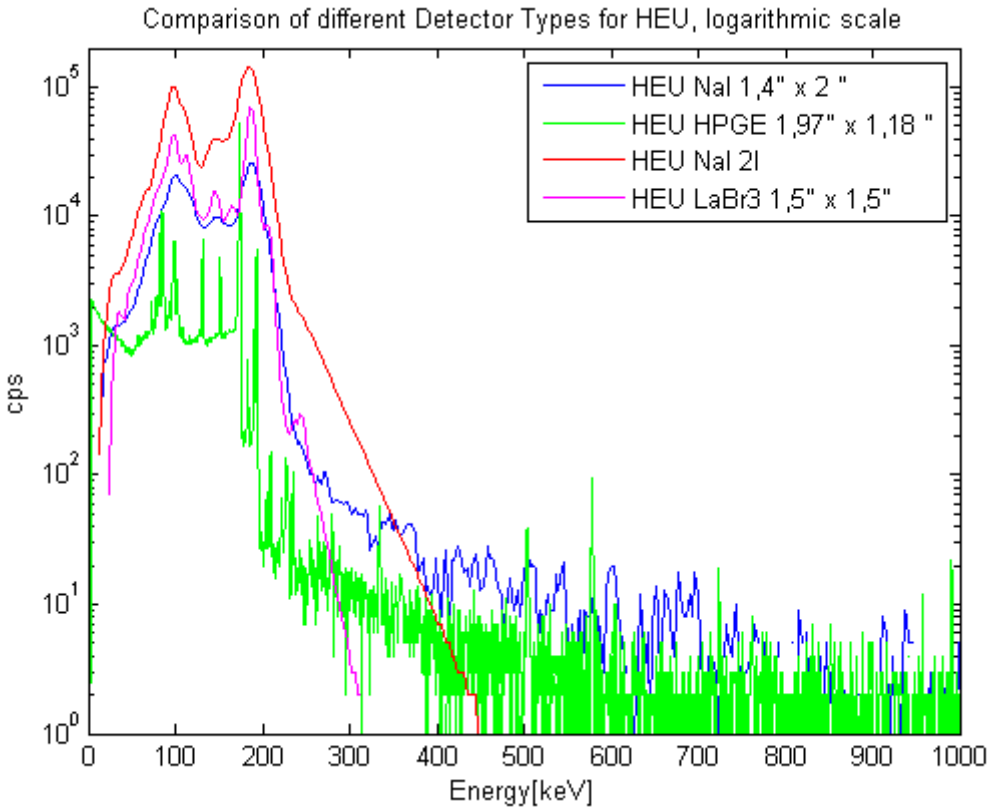

Figure 39: Comparison of 4 different detectortypes for HEU in logarithmic scale

The source envelope could also be the reason for this effect.

3.1 Further steps after the Workshop

After the Workshop all companies were asked to provide their spectra for the next steps of the RASE campaign. This meant that the companies had to subtract the background of each spectrum, add the sensitivity parameter and transform them into the same energy scale. They had as well to convert each spectrum into a n42.42 file format. All of the spectra had to be named the following way: first the name of the company, with 3 characteristic letters, second part the number of the instrument with 3 characteristic numbers, and at the end the characteristic abbreviation for the source. They were also asked to downscale their spectra. With the help of these inputs, the RASE campaign will procede on to its next steps, which will be a spectra acquisition with a temperature and magnetic field influence. After this second spectra acquisition, all of the spectra will be inserted into the provided software, replicated and analyzed as described in the TOR vers. 6.1.

4 Evaluation

After the Base spectra acquisition at the RASE Workshop in Seibersdorf, which is consistent with the first step of RASE, it was necessary to evaluate and verify the ongoing steps. The Evaluation was divided into two parts. The first part was the evaluation of the overlayed spectra, the second part was the evaluation of the dose rate acquisition. One of the aims of RASE is to overlay two or more base spectra and let them be identified by the software of the RIDs. Therefor it must be proven, that these overlayed spectra are consistent with spectra taken with two sources at the same time. This can be verfied by statistical test described in chapter 1. In the following chapters overlayed spectra will be called mixed spectra, spectra created by the software synthetic spectra and spectra taken with the RIDs will be called real spectra. For the purpose of this verification, measurements with the same instruments and the same sources were taken at the same place as the Base spectra acquisition, in a laboratory environment. The chosen sources were Am - 241, Eu - 154 and U - 235. The reason for these specific sources were at the one hand the availability, and at the other hand the sources provide peaks in a broad energy range, compared with peaks at a single place. All of the taken spectra were evaluated and the peak positions, the resolutions and also the counts of the peaks were taken.

4.1 Experimental setup for Evaluation of Spectra

For the experiments the following instruments were used:

- IdentiFINDER Ultra SN 2650 -45
- ORTEC Micro Detective
- ATOMTEX AT 1125
- PRM - 470C/ GN

Besides these instruments, Pb shielding plates, a scale, gloves and tape were used. The chosen sources were:

- Eu - 154; 373300 Bq calibrated on 2/1/2001 Name: 738-64-2
- U - 235; 413 g 89,99%U 235 Name: SU 145 sample ID .900 - 2 (HEU)
- Am - 241; 2,51 MBq calibrated on 15th February 2009 Name: 1317-90-1

First step was to measure the dose rates of the sources at different distances. The dose rates were measured at 10, 20, 50 and 100 cm with and without Pb shielding. In table 39 and 40 the results are shown. No values mean, that the source was no longer measurable or the shielding was to strong. The Δ denominates the error in %

Source/dist.	Am 241	Δ [%]	Eu 154	Δ [%]
10 cm	1,24 μ Sv/h	2	5,2 μSv/h	2
Pb shield	0,082 μSv/h	8	1,39 μSv/h	6
20 cm	0,31 μSv/h	4	1,3 μSv/h	2
Pb shield			0,4 μSv/h	8
50 cm	0,111 μSv/h	8	0,4 μSv/h	8
100 cm			0,24 μSv/h	8

Table 39: Sources and measured DR and CR, part 1

Source/dist.	HEU	Δ [%]	HEU+Am241	Δ [%]
10 cm	2,8 μSv/h	2	4,4 μSv/h	1
Pb shield				
20 cm	0,84 μSv/h	4	1,13 μSv/h	3
Pb shield				
50 cm	0,191 μSv/h	8	0,23 μSv/h	8
100 cm	0,097 μSv/h	8		

Table 40: Sources and measured DR and CR, part 2

of the instrument. For the following measurements a distance of 10 cm was chosen without shielding.
The dose rate measurments were done with the AT 1125. After this step the IdentiFINDER was calibrated for present measurements, the Fine Gain was 1,0410. Background measurement with the AT 1125 gave the following result:

Background		
Count Rate	109	cps
Dose Rate	80	nSv/h

Table 41: Background Measurement

The dose rate was taken with the AT 1125, the count rate with the PRM. The next step was to acquire 10 spectra of Eu - 154/ 152 and Am - 241 and 10 spectra with the mixture Am - 241 and HEU. The sources were placed as shown in picture 40. The spectra were saved in the IndentiFINDER with the numbers 40 - 49 and from 20 - 29. The distance for the measurements were 10 cm, the death time was 8% each measurement was carried out for 60s real time. In picture 41 the placement of the sources is shown.
In figure 42 one of the Am - 241 Eu - 154/152 spectra is displayed, in figure 43 a spectra of the Am - 241 HEU measurements is displayed.
For the verification the spectra had to be generated with the same parameters with the RASE software. The ingoing parameters were the doserates, displayed in table

Figure 40: Experimental setup for spectra Evaluation

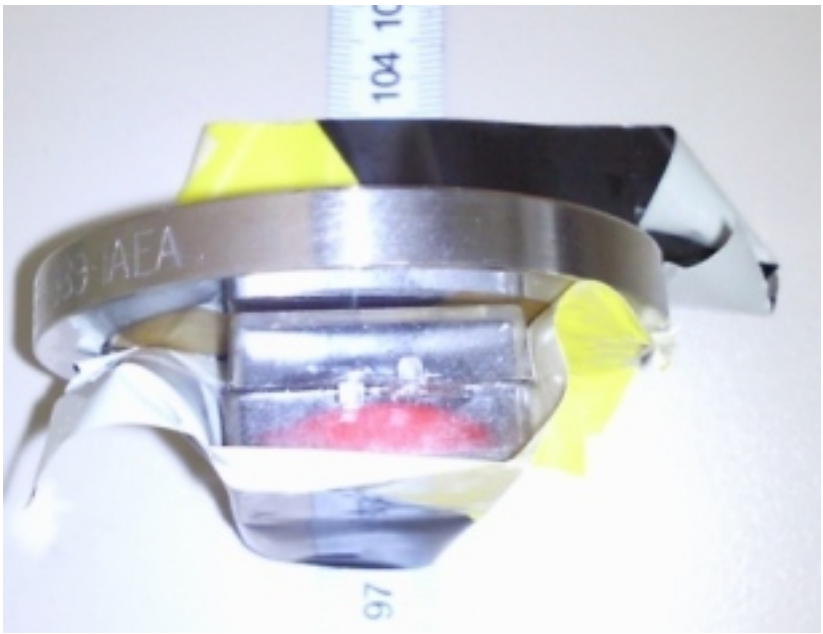

Figure 41: Placement of Sources

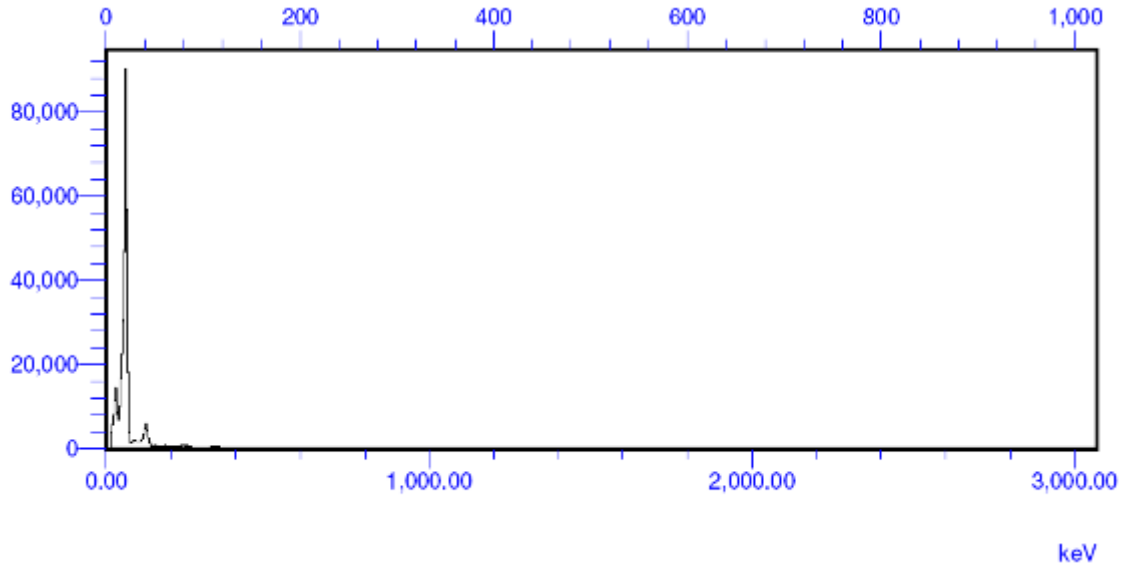

Figure 42: Example of Am - 241 Eu - 154/152 spectrum

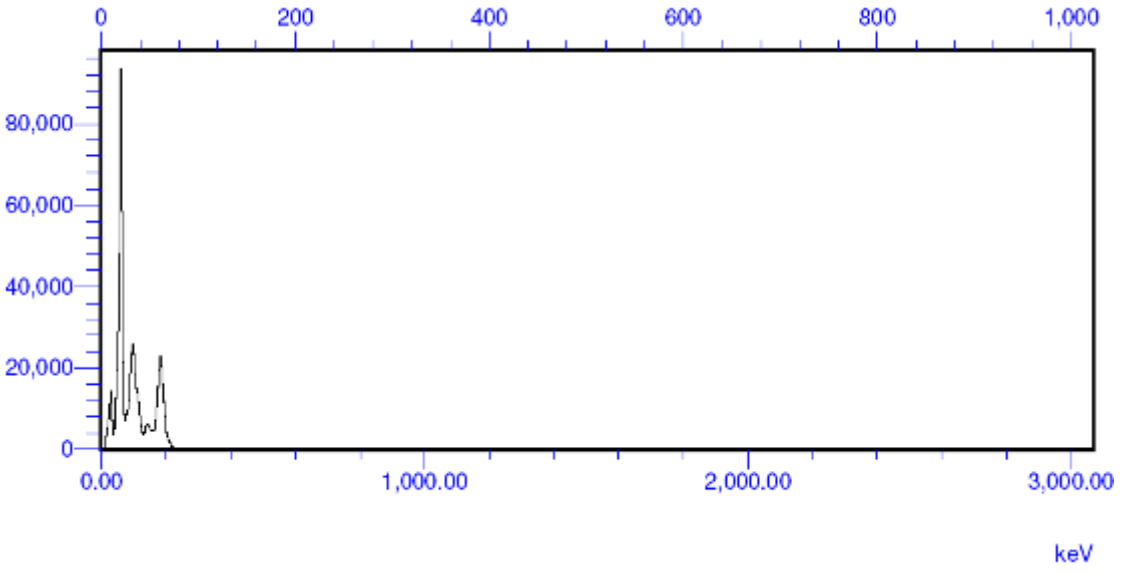

Figure 43: Example of Am - 241 HEU spectrum

?? of the two sources used. The third parameter was the background doserate shown in table 41. The used spectra were the delivered Base spectra of ICX. Ten spectra were generated. In figure 44 a generated Am - 241 Eu - 154 / Eu 152 spectra is shown, and in figure 45 a generated Am - 241 HEU spectra is shown.

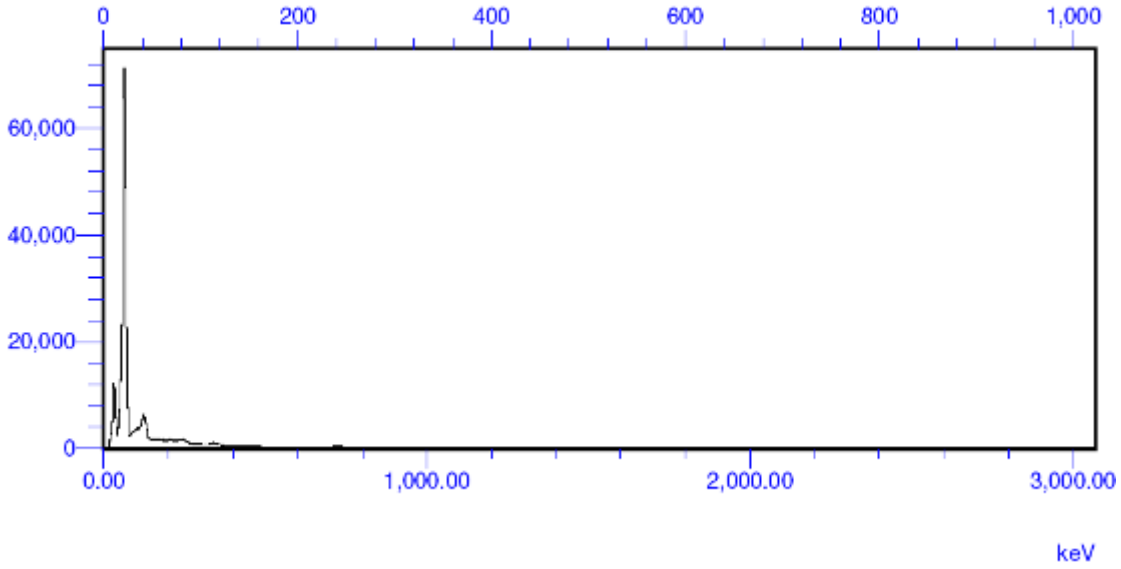

Figure 44: Example of generated Am - 241 Eu - 154/152

To procede with the evaluation parameters had to be chosen. With this choice it is also possible to make a first check of the spectra. The chosen parameter were:

- the centroid of selected peaks
- the resolution of the selected peaks
- the counts of the full spectrum

For the centroid evaluation the peaks had to be chosen after a glance at the spectra. For the Am - 241 Eu 154/ 152 spectra the following peaks shown in table 42 were chosen:

Am - 241	Eu - 154	Eu - 152
59,54 keV	123,14 keV	121,78 keV
	1274,45 keV	344,28 keV
		1408 keV

Table 42: Chosen Peaks for the spectra evaluation of the Am - 241 Eu 154/ 152 spectra

For the Am - 241 HEU Spectra the following peaks shown in table 43 were chosen:

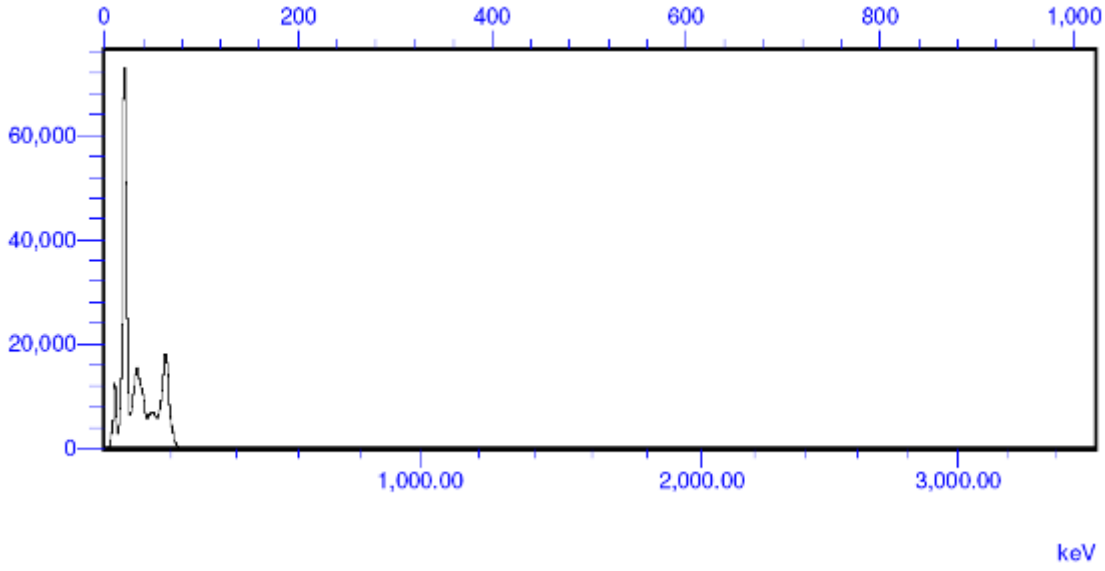

Figure 45: Example of Am - 241 Heu spectrum

Am - 241	HEU
59, 54 keV	99,4keV
	185,72 keV

Table 43: Chosen Peaks for the spectra evaluation of the Am - 241 Eu 154/ 152 spectra

4.1.1 Evaluation for the NaI - Detector

In the following table 44, the centroids of the peaks as well as the resolution parameters read out of the Am - 241 HEU spectra are shown. C_{aq} indicates the centroid of a peak in an aqcuired spectrum, R_{aq} the resolution of peaks in an acquired spectrum, C_{syn}indicates the centroid of a peak in a synthetic spectrum, and R_{syn} is the resolution of the peaks in the synthetic spectra.

Spectrum	Theortical Value [keV]	C_{aq} [keV]	R_{aq} [%]	C_{syn} [keV]	R_{syn} [%]
1	59,54	58,36	17,6	59,33	18,6
	94	94,42		93,95	
	185,72	183,01	11,8	182,85	14,9
2	59,54	58,38	17,6	59,32	18,6
	94	94,41		93,96	
	185,72	183,03	11,7	182,89	15
3	59,54	58,35	17,7	59,33	18,6
	94	92,44		93,95	
	185,72	182,98	11,7	182,91	14,7
4	59,54	58,4	17,8	59,35	18,7
	94	94,38		93,94	
	185,72	183,03	11,8	182,88	14,9
5	59,54	58,41	17,6	59,32	18,6
	94	94,42		93,94	
	185,72	183,08	11,8	182,85	14,9
6	59,54	58,54	17,5	59,33	18,6
	94	94,43		93,95	
	185,72	183,19	11,8	182,9	15
7	59,54	58,41	17,5	59,34	18,6
	94	94,39		93,94	
	185,72	183,08	11,8	182,91	14,9
8	59,54	58,42	17,6	59,33	18,6
	94	94,41		93,93	
	185,72	183,09	11,7	182,94	14,9
9	59,54	58,33	17,7	59,34	18,6
	94	94,48		93,95	
	185,72	182,95	11,8	182,85	14,9
10	59,54	58,38	17,7	59,32	18,7
	94	92,49		93,95	
	185,72	183	11,7	182,87	14,9

Table 44: Centroids and Resolution parameters for the Am - 241 HEU spectra

In the following table 45, the centroids of the peaks as well as the resolution parameters read out of the Am - 241 HEU spectra are displayed. C_{aq} indicates the

centroid of a peak in an acqcuired spectrum, R_{aq} the resolution of peaks in an acquired spectrum, C_{syn} indicates the centroid of a peak in a synthetic spectrum, and R_{syn} is the resolution of the peaks in the synthetic spectra.
After the read out of the centroids, the sum of the peak centroids was calculated and is displayed in table 46 for the Am - 241 Eu - 154/ 152 spectra and in table 47 for the Am - 241 HEU spectra. In both tables the sum_{aq} indicates the Sum of the acquired peaks, the $Rsum_{aq}$ the sum of the resolution parameter, sum_{syn} indicates the sum of the synthetic peaks and $Rsum_{syn}$ the sum of the resolution of the synthetic peaks.
It was necessary to take the sum of the peaks to compensate slight changes in the spectra. With the summation it is also possible to generate a parameter for the whole spectrum and not only for a region or a point. It can easily be seen that the peak positions and the sum of the centroids are similar. There are shifts due to the different detectors used for the base spectra acquisition and for the verification. One can also see, that the shifts are bigger in the real spectra than in the synthetic spectra. One of the reasons is the longer acquiring time for the base spectra, and the random number generator. While the acquired spectra for the evaluation shift between 58,33 keV and 58,54 keV for the Am - 241 peak, the peaks of the synthetic spectra differ only between 59,32 keV and 59,35 keV. For the resolution there is a main difference in the 185,72 peak of the HEU spectrum, the acquired spectra show a resolution around 11,7 %, while the synthetic spectra have a resolution around 15 %. This may be due to different detectors, but should be investigated further. To have a qualitative evaluation a MATLAB based program was written, which takes as input the sums of the peaks, as well as the sum of the resolution parameters. It then uses the synthetic spectra peaks as theoretical values, add them and creates a mean value, does a χ^2 - test and a mean value comparison as described in Chapter 1. The program can be found in the Attachment.
For the χ^2 Test the significance level of 1% was chosen. With one degree of freedom, the value of the χ^2 distribution must be under 6.635 to accept the Zero Hypotheses, which is valid for all data. The only parameter which may be critical, is this under the value of 0,1138. For the mean value comparison, the degrees of freedom are 18, the distribution must be under 2,552 for a significance of 1%, which is given only for the peak positions but not for the resolution parameter. This point was already discussed before and should be investigated further.

4.1.2 Evaluation of the HPGe Detector

It was not possible to do the evaluation for Am - 241 HEU spectra, as the file format of the detector could not be read out. For the Am - 241 Eu - 152/154 spectra it can easily be seen, that the centroids of the different peaks don't vary much. This is due to the characteristic of the detector which has a very good resolution. The second parameter that is displayed is the number of counts under each peak. As it is not possible to read out the resolution, this parameter was chosen as second parameter

Spectrum	Theoretical Value [keV]	C_{syn} [keV]	R_{syn} [%]	C_{aq} [keV]	R_{aq} [%]
1	59,54	58,12	18,3	58,69	17,4
	121,78	121,4	10,7	120,39	12
	1408	1408,23	4,1	1411,52	5
2	59,54	58,11	18,2	58,66	17,7
	121,78	121,38	10,6	120,54	12,2
	1408	1410,68	4,1	1413,98	5,1
3	59,54	58,11	18,2	58,61	17,6
	121,78	121,44	10,6	120,57	12,3
	1408	1411,74	4,8	1413,96	5
4	59,54	58,12	18,2	58,78	17,3
	121,78	121,36	10,6	120,4	12,1
	1408	1413,37	4,6	1412,98	5
5	59,54	58,15	18,2	58,75	17,8
	121,78	121,42	10,7	120,61	12
	1408	1412,34	3,9	1410,42	5,5
6	59,54	58,15	18,3	58,64	17,1
	121,78	121,52	10,6	120,5	12,4
	1408	1410,32	4,3	1410,66	5,7
7	59,54	58,18	18,2	58,45	17,9
	121,78	121,5	10,6	120,38	12,3
	1408	1410,75	4,4	1411,03	5,7
8	59,54	58,15	18,2	58,61	17,9
	121,78	121,5	10,7	120,5	11,9
	1408	1412,66	4,4	1412,19	5
9	59,54	58,16	18,2	58,32	17,9
	121,78	121,49	10,7	120,51	12
	1408	1412,14	4,7	1413,58	5,2
10	59,54	58,13	18,2	58,62	17,6
	121,78	121,42	10,7	120,24	11,9
	1408	1413,81	3,9	1412,06	4,7

Table 45: Centroids and Resolution parameters for the Am - 241 Eu - 154/152 spectra

Number	sum_{aq}[keV]	$Rsum_{aq}$[%]	sum_{syn}[keV]	$Rsum_{syn}$[%]
1	335,79	29,4	336,13	33,5
2	335,82	29,3	336,17	33,6
3	333,77	29,4	336,19	33,3
4	335,81	29,6	336,17	33,6
5	335,91	29,4	336,11	33,5
6	336,16	29,3	336,18	33,6
7	335,88	29,3	336,19	33,5
8	335,92	29,3	336,2	33,5
9	335,76	29,5	336,14	33,5
10	333,87	29,4	336,14	33,6

Table 46: Sum of the peaks for the Am - 241 Eu - 152/154 spectra

Number	sum_{syn}[keV]	$Rsum_{syn}$ [%]	sum_{aq}[keV]	$Rsum_{aq}$[%]
1	1587,75	33,10	1590,60	34,40
2	1590,17	32,90	1593,18	35,00
3	1591,29	33,60	1593,14	34,90
4	1592,85	33,40	1592,16	34,40
5	1591,91	32,80	1589,78	35,30
6	1589,99	33,20	1589,80	35,20
7	1590,43	33,20	1589,86	35,90
8	1589,99	33,20	1589,80	35,20
9	1591,79	33,60	1592,41	35,10
10	1593,36	32,80	1590,92	34,20

Table 47: Sum of the peaks for the Am - 241 HEU spectra

	EuAm	AmU
χ^2 value for		
peaks	0,18	0,008
resolution	2,5	0,414
mean value comparison for		
peaks	2,12	-0,106
resolution	530	-12,1

Table 48: Results of statistical tests

Number	Theoretical Value [keV]	P_{aq}[keV]	R_{aq} [%]	P_{syn} [keV]	R_{syn} [%]
1	59,54	59,77	270	59,96	34519
	121,78	121,91	537	122,09	676
	123,14	123,26	335	123,72	23946
	344,28	344,34	63	344,47	90
	1274,75	1273,51	47	1273,77	65
	1408	1407,02		1407,32	
2	59,54	59,77	271	59,97	34908
	121,78	121,89	526	122,09	1034
	123,14	123,27	313	123,71	23927
	344,28	344,35	63	344,47	91
	1274,75	1273,56	47	1273,74	65
	1408	1407,02		1407,23	
3	59,54	59,77	271	59,97	5272
	121,78	121,89	528	122,09	1086
	123,14	123,27	317	123,62	24885
	344,28	344,34	62	344,44	90
	1274,75	1273,51	47	1273,73	66
	1408	1406,97		1407,31	
4	59,54	59,78	271	59,96	34633
	121,78	121,6	28	122,09	674
	123,14	123,15	168	123,62	23865
	344,28	344,35	61	344,48	90
	1274,75	1273,53	49	1273,77	65
	1408	1407,05		1407,32	
5	59,54	59,77	271	59,98	5262
	121,78	121,62	815	122,09	1044
	123,14	123,15	167	123,62	24134
	344,28	344,35	63	344,46	91
	1274,75	1273,49	47	1273,74	66
	1408	1407,02		1407,25	
6	59,54	59,77	271	59,98	5313
	121,78	121,57	704	122,09	1041
	123,14	123,15	168	123,63	24708
	344,28	344,33	62	344,44	90
	1274,75	1273,55	48	1273,73	66
	1408	1406,98		1407,31	

Table 49: Centroids of the Peaks of HPGe Am - 241 Eu - 152/154 spectra Part 1

Number	Theoretical Value [keV]	P_{aq}[keV]	R_{aq} [%]	P_{syn} [keV]	R_{syn} [%]
7	59,54	59,78	272	59,96	34606
	121,78	121,89	553	122,09	678
	123,14	123,26	324	123,61	23814
	344,28	344,34	63	344,48	90
	1274,75	1273,52	48	1273,77	65
	1408	1407,03		1407,32	
8	59,54	59,78	270	59,98	5228
	121,78	121,62	556	122,09	1066
	123,14	123,13	168	123,62	24242
	344,28	344,35	62	344,46	91
	1274,75	1273,48	47	1273,73	66
	1408	1407,01		1407,25	
9	59,54	59,78	271	59,98	5290
	121,78	121,94	557	122,09	1050
	123,14	123,26	342	123,55	24705
	344,28	344,34	61	344,44	90
	1274,75	1273,52	47	1273,74	66
	1408	1406,96		1407,3	
10	59,54	59,78	271	59,99	5349
	121,78	121,91	531	122,09	869
	123,14	123,27	336	123,55	24355
	344,28	344,33	62	344,45	91
	1274,75	1273,53	47	1273,71	66
	1408	1407,06		1407,26	

Table 50: Centroids of the Peaks of HPGe Am - 241 Eu - 152/154 spectra Part 2

Number	$Psum_{aq}$	$Rsum_{aq}$	$Psum_{syn}$	$Rsum_{syn}$
1	4736,83	1252	4738,65	59296
2	4736,88	1220	4738,44	60025
3	4736,72	1225	4738,47	31399
4	4736,51	577	4738,56	59327
5	4736,42	1363	4738,39	30597
6	4736,33	1253	4738,49	31218
7	4736,85	1260	4738,55	59253
8	4736,38	1103	4738,38	30693
9	4736,76	1278	4738,4	31201
10	4736,94	1247	4738,31	30730

Table 51: Sum of Peaks and resolution for HPGe spectra of Am - 241 Eu 152/154

Ortec	Peaks	counts
χ^2 value	10000	2,0075
mean value comparison	63,73	0,0004

Table 52: Results of statistical tests for ORTEC

of evaluation. There is a huge difference between the counts of the acquired spectra for the evaluation and the synthetic spectra. The ongoing evaluation was similar to the evaluation of the NaI detectors. In table 52 the results of the χ^2 and the mean value comparison are shown. Due to the characteristics of the detector, it could be expected that both test would fail. The levels for the failure are the same as for the NaI - detector analysis. Especially the peak position evaluation shows a big difference. A further investigation and evaluation of this point is necessary to assure the correctness of the program.

4.2 Experimental Evaluation of Sensitivity Parameter Calculations

The sensitivity parameter is defined by

$$S = \frac{cps}{\mu Sv/h}$$

It is one of the most important parameters in the RASE program. With this value each instrument has a characteristic value for the spectra which are created. This means, that with the help of this parameter spectra can be created with every dose rate. So the evaluation of this parameter is very important. It must be verified, that even if two spectra are mixed, the sensitivity parameter is correct in the created spectrum. The experiment was done at the ATI in Vienna. The sources used for this evaluation were a Am - 241, a Eu - 154, a Co - 60 and a DU source. In table 53 the information on the sources is given.

Source	Activity	Information
Eu - 154	unknown	26,5μSv/h at 21cm
DU		0,4% enriched, 7,554 kg , 2,01μSv/h at 21 cm
Co - 60	27 MBq	38,5μSv/h at 21 cm
Am -241	3,7Gbq	33μSv/h at 21 cm

Table 53: Information on sources for Sensitivity parameter validation

The experiment was carried out with the IdentiFINDER Ultra in gamma count mode. The dose rate was taken with the Thermo FH 40 G Doseratemeter. It is a gamma meter with an intern proportional counter tube. The sources were placed at a distance of 25 cm to the detector at the exact heigth of the detector. In the following table, the results of the measurements are shown. CR indicates the count rate, DR the dose rate, and cps are the counts per seconds.

Sources	time [s]	CR	DR[μSv/h]	cps
Am - 241	60	571613	25,8	95694
DU	60	112466	1,36	1874
Eu - 154	60	884641	24	14744
Co - 60	60	1424841	37,8	23747

Table 54: Measurement results for sensitivity parameter validation part 1

To evaluate the sensitivity parameter S, it was calculated with the measured results after equation 8. For the synthetic spectra, spectra with the same parameters wer generated, and in the editor mode, one can find at the end the sensitivity, as shown in the picture 46. The ingoing parameters were for the single spectra, shown in table 55:

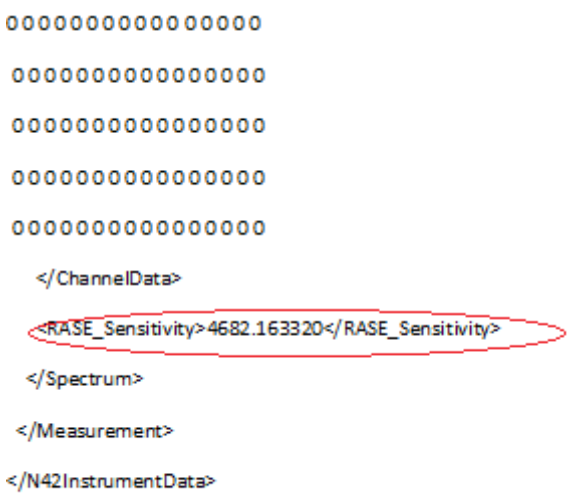

Figure 46: Sensitivity in Rase generated spectra

	DR[μSv/h]	time [s]
Am - 241	25,8	60
DU	1,36	60
Eu - 154	24	60
Co - 60	37,8	60
Background	0,102	

Table 55: Ingoing parameters for sensitivity evaluation

Sources	S_{rase}	S_{meas}
Am - 241	4682	3709
DU	1310	1378
Eu - 154	822	614
Co - 60	442	628

Table 56: Results for Sensitivity parameter calculation

The results for the sensitivity are listed in table 60. S_{rase} is the Sensitivity read out of the RASE files, S_{meas} is the calculated Sensitivity after the measurements.
The next step was to evaluate the Sensitivity parameters of two mixed spectra. The same steps as described above were carried out, with the only difference, that this time two sources were measured together. Again there were ingoing parameters, shown below in table 57.

	DR[μSv/h]	time [s]
Am - 241 + Eu - 154	45,4	60
Co - 60 + DU	38	60
Background	0,102	

Table 57: Ingoing parameters for Sensitivity evaluation of mixed spectra

In table 58 and in table 59 the results are shown.

Sources	time[s]	CR	DR[μSv/h]	cps
Am - 241 + Eu - 154	60	5960259	45,4	99338
Co - 60 + DU	60	1544777	38	25746

Table 58: Measurement results for Sensitivity parameter calculation part 2

Sources	S_{rase}	S_{meas}
Am - 241 + Eu - 154	2824	2188
Co - 60 + DU	472	678

Table 59: Results of Sensitivity parameter for mixed sources

4.2.1 Comparison of Sensitivity parameter evaluation

The results of the Sensitivity parameter evaluation for single spectra are shown in table 60. For mixed spectra they are written in table 59. As it is almoust impossible to simulate the real situation, the results can be considered as very good. The deviation depends on the source, but all results are in the same order of magnitude. The deviations can be explained by problems of creating the exact same measurement situation, starting with the source. The Eu - 154 source taken for the RASE spectra has also parts of Eu - 152 in it, so it reacts differently for the counts as the source taken for the validation. Another problem was the Dose rate measurement. The Thermo Doserate meter has a long integrating time, and does not always show constant values. At the RASE Workshop a AT 1125 was taken for count rate measurements, this instrument was not available at the ATI. To conclude this evaluation, it can be said that the sensitivity parameter in the RASE program can be taken as a characteristic value for the spectra.

5 Conclusion

The aim of this work was to describe and evaluate the RASE Program of the IAEa. RASE - Replicative assessment of spectrometric Equipment is a semi - empirical approach for performance evaluation of radionuclide detection equipment, which consists of 6 steps:

- Base spectra acquisition

  A limited number of materials and sources containing high risk materials were acquired with high statistical accuracy in laboratory enviroment - Base Spectra.

- Quantitative assesment of hardware tolerance

  The Influence of factors as temperature factors and magnetic field are assessed.

- Replication

  A large number of spectra is replicated using the base spectra - Sample Spectra.

- Injection and Identification

  The sample spectra are injected into the software of the instruments and the spectra are identified.

- Indentification results interpretation

  A database for the results of the identification is created and 2D or 3D plots can be gathered.

- Validation.

  The validation of the program has to be done.

A more detailed description can be found in chapter 1.5 . The first step, Base spectra acquisition, which is the main topic to this work, was carried out in December 2009 at the Seibersdorf Laboratory and the Institute of Atomic and Subatomic Physics (ATI) in Vienna. It will be continued in spring 2011 at the ATI. The report of this workshop may be found in chapter 2.
After the Base spectra acquisition an evaluation of the ongoing procedures was necessary. This was at the one hand the evaluation of overlaying or mixing spectra synthetically. This evaluation was done with two statistical tests, a χ^2 test and a mean value comparison. The results of this evaluation are shown in table 48. For the NaI - detector this means that there is no difference between the synthetic and the real spectra, for the sum of the peak positions with a probability of 1%. For the resolution parameter problems occured, which are described in Chapter 3. Also for the HPGe detector the evaluation showed thath due to the instruments characteristics the spectra are not equal. This point should be investigated further.

But, however, this has no influence in the indentification results of the instruments, as the instruments use also other parameter for the indentification of radionuclides than peak positions. The second part of the evaluation was the sensitivity parameter evaluation. Results for this very important parameter are shown in table 61 and 60. The sensitivity parameter is therefor a valid parameter for the spectra. The results are displayed in the tables below.

Sources	S_{rase}	S_{meas}
Am - 241	4682	3709
DU	1310	1378
Eu - 154	822	614
Co - 60	442	628

Table 60: Results for Sensitivity parameter calculation

Sources	S_{rase}	S_{meas}
Am - 241 + Eu - 154	2824	2188
Co - 60 + DU	472	678

Table 61: Results of Sensitivity parameter for mixed sources

6 References

1. RASE, Replicative assessment of spectrometric equipment,Reference Manual, Ver. 6.2 SGTS - IAEA, Vienna, Austria (2009)

2. R. Arlt, K. Baird, J. Blackadar, C. Blessenger, D. Blumenthal, P.Chiaro, K. Frame, E. Mark, M. Mayorov, M. Milovidov, R. York, Semi-Empirical Approach for Performance Evaluation of Radionuclide Identifiers, Proceedings of the IEEE Nuclear Science Symposium,Orlando, USA (2009)

3. Glenn F.Knoll, Radiation Detection and Measurement 4^{th} Edition: John Wiley & Sons, Inc.,Michigan, USA, ISBN 978-0-470-13148-0 (2010)

4. G.Gilmore, J.D. Hemingway, Practical Gamma-Ray Spectrometry:John Wiley & Sons, Inc. Warrington, UK, ISBN 0-471-95150-1 (1995)

5. Combating illicit trafficking in nuclear and other radioactive material: Technical guidance, reference manual, IAEA, Vienna, Austria, ISBN 978-92-0-109807-8 (2007)

6. B.Siebenhofer, "Meaning of the Confidence Index displayed on Radionuclide Identification Devices and Spectrometric Personal Radiation Detection"", Master theses, Vienna University of Technology , Austria (2009)

7. V. Kleinrath, "A study of Gamma Interference Scenarios for Nuclear Security Purposes", Master theses,Vienna University of Technology , Austria (2010)

8. M. Gerstmayr, Theoretical and Experimental support of the RASE*programme to optimize boarder monitoring equipment for illicit trafficing prevention", Master theses,Vienna University of Technology , Austria (2011)

9. W.v.d.Linden, A. Prüll, Lecture course book: "Wahrscheinlichkeitstheorie, Statistik und Datenanalyse", University of Technology, Graz, Austria (2001)

10. H. Rabitsch, Lecture course book: "Strahlenschutz", University of Technology, Graz, Austria (2007)

11. R.Kahn, S.Karimsadeh, H.Böck, M.Villa, "Triga Fuel Burn-up Calculations Supported by Gamma Scanning", Vienna University of Technology, Austria

12. www.mirion.com - Product Info

13. www.radiation.icxt.com - Product Info

14. www.tsasystems.com - Product Info

15. www.atomtex.com - Product Info

16. www.canberra.com - Product Info, 2008

17. www.ortec-online.com - Product Info

18. www.aspect.dubna.ru - Product Info

19. FLUKE Biomedical, Victoreen® 451B & 451B-DE-SI Ion Chamber Survey Meter, Operators Manual, September 2009

20. http://tsasystems.com/ - Product Info

7 Attachment

7.1 Information on Sources

In the following tables one can find relevant information on the used isotopes. For each isotope there is the half Live, the number of decays and the type of decay, the branching ratio if there is more than one sort of decay, the daughter products and the main Gamma Energy Lines, which appear in the spectra. At the end of each table, there is also a decay schema.

- Am - 241 Used in smoke detectors, to measure levels of toxic lead in dried paint samples, to ensure uniform thickness in paper production and for moisture gauges
- Ba - 133 Used in portable gauges to detect void spaces
- Cf - 252 A neutron sources used for well logging in oil field exploration, to gauge moisture content of soil in road construction and building industries, and to measure moisture of material stored in silos
- Cm - 244 Used in mining industry to analyse material excavated from drilling operations and gauging
- Co - 60 Used for teletherapy, gamma radiography, gauging, to sterilize surgical instruments and too preserve poultry, fruits and spices
- Cr - 51 Used for research purposes in red blood cell survival studies
- Cs - 137 Used for gamma radiography, gauging, to treat cancer, to measure and control the liquid flow in oil pipelines, filling level of food, drugs and other products
- Eu - 152 and Eu - 154 The primary use of Europium is in nuclear reactor control rods. Europium-doped plastics have been used as laser materials, and Europium Oxide serves as a Phosphor activator. Europium has been used to activate Yttrium Vanadate for its use in the red Phosphors of color television tubes.
- F - 18 It is used as a radiopharmaceutical for PET
- Ga - 67 Used for localization of inflammations and tumors
- I - 123 Used in nuclear medicine imaging, including single photon emission computed tomography (SPECT).
- I - 125 Widely used to diagnose thyroid disorders
- I - 131 Used to diagnose and treat thyroid disorders

- In - 111 Used in indium leukocyte imaging, or indium scintigraphy.
- Ir - 192 Used for gamma radiography to test the integrity of pipeline welds, boilers and aircraft parts and in brachytheraphie
- K - 40 Potassium is used as a fertilzer
- Pu - 238 Used for pacemakers, space applications, radioisotopic thermoelectric generators(RTG) and portable gauges
- Ra - 226 Used in the past in many different applications such as luminous paint, brachytherapy and radiography
- Se - 75 Used in protein studies in life science research and in radiography
- Sm - 153 Used to treat pain
- Sr - 90 Used in RTGs, thickness gauges, calibration, medical treatment(brachytherapy)
- Tc -99m The most widely used radionuclide for diagnostic studies in nuclear mdeicine. Different chemical forms are used for brain, bone, liver, spleen and kidney imaging and also for blood flow studies
- Th - 232 in thoriated tungsten, used in electric welding rods in the construction, aircraft, petrochemical and food processing equipment industries. Ensures easier starting, greater stability and less metal contamination.
- Tl - 201 Used for heart scintigraphy
- Tm - 170 used for portable X-Ray machines, and may be used in cancer theraphy
- U - 235 Fuel for NPPs and naval nuclear propulsion systems, also used to produce fluorescent glassware, a variety of coulored glazes and wall tiles
- U - 238 Used as γ-shielding material, weight balance in aircraft an ships
- Xe - 133 Used in nuclear medicine for lung ventilation and blood flow studies
- Yb - 169 used for medical applications

7.2 Information on Decays of Nuclides

EP indicates the emission probability.

Am - 241			
Half Live	433 a		
Number of decays	2		
	α	SF	
branching ratio	1	$3{,}77*10^{-12}$	
Daughter product	Np - 237		
Gamma lines for Am - 241			
gamma lines [keV]	EP [%]	X-Ray lines [keV]	EP [%]
59,536	35,9	14,4	36,49
26,34	2,4	4,608	7,15
Decay scheme	Am - 241	$\Downarrow$	
	α	$\downarrow$	
	Np - 237	$\downarrow$	
	$\downarrow$		
	Neptunium series		

Table 62: Am - 241

Ba - 133			
Half Live	10,53 a		
Number of decays	1		
	β^+		
branching ratio	1		
Daughter product	Cs - 133 stable		
Gamma lines [keV]	EP [%]	X-Ray lines [keV]	EP [%]
356,017	62,05	30,972	64,9
80,997	34,1	30,625	35,1
302,853	18,33	35	23,3
383,851	8,94	4,29	17
276,398	7,164		
79,623	2,62		
53,161	2,199		
Decay scheme		$\swarrow$ β^+Ba - 133	
	Cs - 133		

Table 63: Ba - 133

Cf - 252		
Half Live	2,65 a	
Number of decays	2	
	α	SF
branching ratio	0,969	$3{,}09*10^{-2}$
Daughter product	Cm - 248	
X-Ray lines for Cf - 252 [kev]	EP [%]	
15,517	5,48	
5,036	1,378	
Decay scheme	Cf 252	$\Downarrow$
	(α)	$\downarrow$
	Cm - 248	$\downarrow$
	$\downarrow$	
	Thorium series	

Table 64: Cf - 252

Cm - 244		
Half Live	18,11 a	
Number of decays	2	
	α	SF
branching ratio	1	1,34E-06
Daughter product	Pu - 240	
X-Ray lines for Cm-244 [keV]	EP [%]	
14,792	8,05	
4,756	1,76	
Decay scheme	Cm - 244	$\downarrow$
	(α)	$\downarrow$
	Pu - 240	$\downarrow$
	$\downarrow$	
	Thorium series	

Table 65: Cm - 244

Co - 60	
Half Live	5,27 a
Number of decays	1
	β^-
branching ratio	1
Daughter product	Ni - 60 stable
Gamma lines [keV]	EP [%]
1332,5	99,98
1173,2	99,9

Table 66: Co - 60

Cr - 51			
Half Live	27,7 d		
Number of decays	1		
	β^+		
branching ratio	1		
Daughter product	V - 51 stable		
Gamma lines [keV]	EP [%]	X-Ray lines[keV]	EP[%]
320,08	9,83	4,952	13,08
		4,944	6,59
		5,43	2,61

Table 67: Cr - 51

Cs - 137			
Half Live	30,02 a		
Number of decays	2		
	β^-	β^-	
branching ratio	0,054	0.946	
Daughter product	Ba - 137	Ba - 137m	
E_{max}	511,553 (94,6 %)	1173,2 (5,4 %)	
Gamma lines for Ba - 137 m			
Gamma lines [keV]	EP [%]	X-Ray lines [keV]	EP [%]
661, 645	89,92	32,193	3,8
		31,817	2,06
		4,544	1,3
		36,4	1,13
Decay scheme	Cs - 137 (β)	$\rightarrow$	Ba - 137 m
		$\downarrow$	$\downarrow$ (γ)
		$\hookrightarrow$	Ba 137

Table 68: Cs - 137

Eu - 152			
Half Live	13,33 a		
Number of decays	2		
	β^-	β^+	
branching ratio	0,2792	0,7208	
Daughter product	Gd - 152	Sm - 152 stable	
γ-lines for Eu-152[keV]	EP [%]		
121,78	28,38		
344,28	26,58		
1408	20,85		
964,13	14,49		
1112,1	13,56		
778,91	12,96		
1085,9	9,92		
244,7	7,51		
867,39	4,21		
443,98	2,8		
411,11	2,23		
1089,7	1,71		
1299,1	1,62		
1212,9	1,39		
Gd-152(α)Sm-148	Nd-144 $\rightarrow$	stable	
$\rightarrow$ Sm-148(α)	Nd-144(α)Ce-140		

Decay scheme		$\swarrow(\beta^+)$Eu 152($\beta^-)\searrow$	
	Sm - 152		Gd - 152$\downarrow$
			(α) $\downarrow$
			Sm - 148$\downarrow$
			(α) $\downarrow$
			Nd - 144$\downarrow$
			(α) $\downarrow$
			Ce - 140 $\downarrow$

Table 69: Eu - 152

Eu 154			
Half Live	8,61 a		
Number of decays	2		
	β^-	β^+	
branching ratio	0,9998	0,0002	
Daughter product	Gd 154 stable	Sm 154 stable	
Gamma lines for Eu 152 [keV]	EP [%]		
123,14	40,5		
1274,45	35,5		
723,3	19,7		
1004,76	17,4		
873,19	11,5		
996,32	10,3		
248,04	6,59		
591,74	4,48		
756,87	4,34		
692,41	1,7		
1596,48	1,67		
Decay scheme	$\swarrow$	(β^+)Eu 154(β^-)	$\searrow$
	Sm 154		Gd 154

Table 70: Eu - 154

F - 18	
Half Live	1,83 h
Number of decays	1
	β^+
branching ratio	1
Daughter product	O - 18 stable
X-Ray lines [keV]	EP [%]
511	200

Table 71: F - 18

Ga - 67			
Half Live	3,26 d		
Number of decays	1		
	β^+		
branching ratio	1		
Daughter product	Zn - 67 stable		
Gamma lines [keV]	EP [%]	X-ray lines[keV]	EP [%]
93,311	37	8,639	32
184,577	20,4	8,616	16,5
300,219	16,6	9,57	6,6
393,529	4,64		
91,266	2,96		
208,951	2,33		

Table 72: Ga - 67

I - 123			
Half Live	13,19 h		
Number of decays	1		
	β^+		
branching ratio	1		
Daughter product	Te - 123		
Gamma lines for I - 123			
Gamma lines [keV]	EP [%]	X-Ray lines [keV]	EP [%]
158,97	83,3	27,47	46,1
528,96	1,39	27,2	24,7
		31	16
		3,77	9,4
Te - 123	Half Live	$1*10^{13}$ a	
X-Ray lines for Te - 123			
X- Ray lines [keV]	EP [%]		
3,6	6,04		
Decay scheme			$\swarrow(\beta^+)$ I - 123
		$\swarrow$ (β^+) Te - 123	
	Sb - 123 (stable)		

Table 73: I - 123

I - 131			
Half Live	8,04 d		
Number of decays	2		
	β^-	β^-	
branching ratio	0,98914	0,8069	
Daughter product	Xe - 131 stable	Xe - 131 m	
Gamma lines for I - 131			
Gamma lines [keV]	EP [%]	X-Ray lines [keV]	EP [%]
364,48	81,24	29,779	2,54
636,973	7,27	29,458	1,369
284,298	6,05		
80,182	2,62		
722,893	1,8		
Xe - 131 m	Half Live 11,9 d	IT decay to Xe - 131	
Gamma lines for Xe - 131 m			
Gamma lines [keV]	EP [%]	X-Ray lines [keV]	EP [%]
163,93	1,96	29,779	28,144
		29,458	15,17
		33,6	10
		4,11	8,2
Decay scheme	I- 131 (β^-)	$\searrow$	
	$\downarrow$	Xe - 131 m	
	$\downarrow$	(γ)	
	$\hookrightarrow$	Xe - 131	

Table 74: I - 131

In - 111			
Half Live	2,38 d		
Number of decays	2		
	β^+	β^+	
branching ratio	0,5	0,5	
Daughter product	Cd - 111 stable	Cd - 111 m	
Gamma lines for In - 111			
Gamma lines [keV]	EP [%]	X-Ray lines [keV]	EP [%]
245,35	94	23,174	44,59
171,28	90,2	22,984	23,63
		26,1	14,6
		3,13	7,08
Cd - 111 m	Half Live 4,86 min		
Gamma lines for Cd - 111m			
Gamma lines [keV]	EP [%]	X-Ray lines [keV]	EP [%]
245,395	94	23,174	27,38
150,825	30,3	22,98	14,57
		26,09	7,47
		3,157	6,98
		26,64	1,45
Decay scheme	↙	(β^+)In - 111	
	Cd - 111 m	↓	
	(γ)	↓	
	Cd - 111	↩	

Table 75: In - 111

Ir - 192			
Half Live	73,83 d		
Number of decays	2		
	β^-	β^+	
branching ratio	0.954	0.046	
Daughter product	Pt - 192 stable	Os - 192 stable	
Gamma lines for Ir - 192			
gamma lines [keV]	EP [%]	X-Ray lines [keV]	EP [%]
316,5	83	66,832	4,63
468,1	47,7	94,4	4,2
308,5	29,75	65,122	2,7
296	28,73	75,7	2,01
604,4	8,09	63	2,01
612,5	5,26	8,91	1,51
588,6	4,48	61,486	1,16
205,8	3,18		
484,6	3,14		
Decay scheme	↙	(β^+) Ir - 192 (β^-)↘	
	Os - 192		Pt - 192

Table 76: Ir - 192

K 40		
Half Live	1,281* 109 years	
Number of decays	2	
	?-	?+
branching ratio	0,893	0,107
Daughter product	Ca 40 stable	Ar 40 stable
Gamma lines for K 40		
Gamma lines [keV]	EP [%]	
1460,8	107	

Table 77: K - 40

Pu - 238			
Half Live	87,76 a		
Number of decays	2		
	SF	α	
branching ratio	1,86E-09	1	
Daughter product		U - 234	
		Thorium-Radium Reihe	
Gamma lines [keV]	EP [%]	X-Ray lines [keV]	EP [%]
99,853	0.0735	14,091	10,1
152,72	0.00127	44,63	1,99

Table 78: Pu - 238

Ra 226	
Half Live	1600 a
Number of decays	1
	α
branching ratio	1
Daughter product	Rn 222
Gamma lines for Ra 226	
Gamma lines [keV]	EP [%]
185,99	3,28
Decay scheme	Ra 226 $\downarrow$
	(α) $\downarrow$
	Rn 226$\downarrow$
	$\downarrow$
	Radium series

Table 79: Ra - 226

Se - 75			
Half Live	120 d		
Number of decays	1		
	β^+		
branching ratio	1		
Daughter product	As - 75 stable		
Gamma lines[kev]	EP [%]	X Ray lines[kev]	EP [%]
264,66	59,1	10,54	33,35
136	58,98	10,51	17,11
279,54	25,18	11,7	7,72
121,12	17,32		
400,66	11,56		
96,734	3,48		
198,6	1,47		
303,92	1,34		
66,06	1,14		

Table 80: Se - 75

Sm - 153			
Half Live	1,95 d		
Number of decays	1		
	β^-		
branching ratio	1		
Daughter product	Eu - 153 stable		
Gamma lines [keV]	EP [%]	X-Ray lines [keV]	EP [%]
103,18	28,3	41,54	31,28
69,67	5,25	40,9	17,3
		47	12,24
		5,85	11,84

Table 81: Sm - 153

Sr - 90			
Half Live	29,14 a		
Number of decays	1		
	β^-		
branching ratio	1		
Daughter product	Y - 90		
E_{max}	546 keV		
Y - 90 energies for	Gamma energies		
gamma lines [keV]	EP [%]		
1760,7	0.016		
Decay scheme	Sr - 90 $(\beta^-)\searrow$		
		Y - 90 $(\beta^-)\searrow$	
			Zr - 90

Table 82: Sr - 90

Tc - 99m			
Half Live	6 h		
Number of decays	2		
	β^-	IT	
branching ratio	3,70E-05	0,999963	
Daughter product	Ru - 99 stable	Tc 99	
gamma lines for Tc - 99m			
Gamma lines [keV]	EP [%]	X-Ray lines [keV]	EP [%]
140,466	88,97	18,367	3,745
		18,251	1,97
Tc 99 is a pure β-emitter			

Decay scheme	Tc - 99 m (β^-)$\rightarrow$		
	(γ)	$\downarrow$	
	Tc - 99(β^-)	$\downarrow$	
	$\hookrightarrow$	Ru - 99	

Table 83: Tc - 99m

Th - 232		
Half Live	$1,41 * 10^{10} a$	
Number of decays	2	
	α	SF
branching ratio	1	$1,4 * 10^{-11}$
Daughter product	Ra - 228	
X-Ray lines for Th - 232		
X-Ray lines [keV]	EP [%]	
12,742	8,12	
3,891	1,27	

Decay scheme	Th - 232	$\downarrow$
	(α)	$\downarrow$
	Ra - 228	$\downarrow$
	$\downarrow$	
	Thorium series	

Table 84: Th - 232

Tl - 201			
Half Live	3.04 d		
Number of decays	1		
	β^+		
branching ratio	1		
Daughter product	Hg - 201 stable		
Gamma lines [keV]	EP [%]	X-Ray lines [keV]	EP [%]
1,57	40,28	70,819	47,3
167,43	10,6	9,99	46
135,34	2,798	68,895	27,8
		80,3	20,8

Table 85: Tl - 201

Tm - 170			
Half Live	129 d		
Number of decays	2		
	β^-	β^+	
branching ratio	0,99854	0,00146006	
Daughter product	Yb - 170 stable	Er - 170 stable	
Gamma lines [keV]	EP [%]	X-Ray lines [keV]	EP [%]
84,257	3,255	7,42	4,03
		52,389	2,24
		51,354	1,27
Decay scheme	↙	(β^+)Tm 170(β^-)↘	
	Er - 170		Yb - 170

Table 86: Tm - 170

U 235		
Half Live	$7,0428 * 10^7$ years	
Number of decays	2	
	α	SF
branching ratio	1	2*E-10
Daughter product	Th 231	
Gamma lines for U 235		
Gamma lines [keV]	EP [%]	EP [%]
185,72	57,24	43,79
143,76	10,96	8,37
163,33	5,08	6,13
205,31	5,01	3,75
109,16	1,53	1,35
202,11	1,08	
Th 231	Half Live:	1.06 days
Gamma lines for Th 231		
Gamma lines [keV]	EP [%]	EP [%]
25,64	14,60	77,61
84,214	6,71	15,69
Decay scheme	U 235	$\downarrow$
	(α)	$\downarrow$
	Th 231	$\downarrow$
	$\downarrow$	
	Uran - Actinium series	

Table 87: U - 235

U 238			
Half Live	$4.471 * 10^9$ years		
Number of decays	2		
	α	SF	
branching ratio	0,999999	5.4 E-07	
Daughter product	Th 234		
Gamma lines for U 238			
X - Ray lines [keV]	EP [%]		
13,409	8,37		
4,176	1,52		
Th 234	Half Live:	24.1 days	
Gamma lines for Th 234			
Gamma lines [keV]	EP [%]	X-Ray lines [keV]	EP [%]
63,29	4,00	13,746	9,37
92,38	2,72	4,319	1,77
92,8	2,688		
Decay scheme	U 238	$\downarrow$	
	(α)	$\downarrow$	
	Th 234	$\downarrow$	
	$\downarrow$		
	Uran - Radium series		

Table 88: U - 238

Xe - 133			
Half Live	5,25 d		
Number of decays	1		
	β^-		
branching ratio	1		
Daughter product	Cs - 133 stable		
Gamma lines [keV]	EP [%]	X-Ray lines [keV]	EP [%]
81	37,1	30,973	15,45
		30,625	8,347
		35	5,55
		4,29	3,8

Table 89: Xe - 133

Yb - 169			
Half Live	32,01 d		
Number of decays	1		
	β^+		
branching ratio	1		
Daughter product	Tm - 169 stable		
Gamma lines [keV]	EP [%]	X-Ray lines [keV]	EP [%]
63,119	41,64	50,742	54,14
197,95	35,9	7,18	30,97
177,21	22,33	49,773	30,69
109,78	17,41	57,5	22,27
130,52	11,48		
307,73	9,87		
93,613	2,54		
118,19	1,91		
261,07	1,68		

Table 90: Yb - 169

7.3 MATLAB program

```
A = xlsread('AmUpeaksICX',1,'G2:J11')
D = A(:,1);
E = A(:,2);
B = A(:,3);
C = A(:,4);
a1 = B(1); a2 = B(2); a3 = B(3); a4 = B(4); a5 = B(5); a6 = B(6); a7 = B(7); a8
= B(8); a9 = B(9); a10 = B(10);
av = [a1 a2 a3 a4 a5 a6 a7 a8 a9 a10];
a = mean(av);
b1 = C(1); b2 = C(2); b3 = C(3); b4 = C(4); b5 = C(5); b6 = C(6); b7 = C(7); b8
= C(8); b9 = C(9); b10 = C(10);
bv = [b1 b2 b3 b4 b5 b6 b7 b8 b9 b10];
b = mean(bv);
var1 = [D(1) E(1)]; var2 = [D(2) E(2)];
var3 = [D(3) E(3)]; var4 = [D(4) E(4)];
var5 = [D(5) E(5)]; var6 = [D(6) E(6)];
var7 = [D(7) E(7)]; var8 = [D(8) E(8)];
var9 = [D(9) E(9)]; var10 = [D(10) E(10)];
vara = var(av);
varb = var(bv);
av = a;
bv = b;

chi = ((var1-[a b]).^2)./[av bv] + ((var2-[a b]).^2)./[av bv]+((var3-[a
b]).^2)./[av bv]+((var4-[a b]).^2)./[av bv]+((var5-[a b]).^2)./[av bv]...
   ...+((var6-[a b]).^2)./[av bv]+((var7-[a b]).^2)./[av bv]+((var8-[a
b]).^2)./[av bv]+((var9-[a b]).^2)./[av bv]+((var10-[a b]).^2)./[av bv]

varvecv = [var1 ; var2; var3; var4; var5; var6; var7; var8; var9; var10];
avec = [a1 ; a2; a3; a4; a5; a6; a7; a8; a9; a10];
bvec = [b1 b2 b3 b4 b5 b6 b7 b8 b9 b10]';
L1 = length(avec);
L2 = length(varvecv);
avec = [avec bvec];
L = L1+L2;
deltab1 = 1./L1.*sum(avec);
deltab2 = 1./L2.*sum(varvecv);
veca = [a1 ; a2; a3; a4; a5; a6; a7; a8; a9; a10];
test1 = avec - (ones(10,1)*deltab1);
test2 = varvecv - (ones(10,1)*deltab2);
test1 = test1.^2;
test2 = test2.^2;

deltad1 = 1./L1.*sum(test1)
deltad2 = 1./L2.*sum(test2)
delta = abs(deltab1 - deltab2)
sigma = L/(L1*L2)*(L1*deltad1+L2*deltad2)
t = sqrt(L-2)*delta./(sigma)
```